POSTER SESSIONS

POSTER SESSION

PARTITIONING

M.J. Hudson (University of Reading)

STUDIES ON BEHAVIOUR OF SELENIUM AND ZIRCONIUM IN PUREX PROCESS

J.A. Suárez, G. Piña, A.G. Espartero, A.G. de la Huebra
CIEMAT, Dpto. de Fisión Nuclear, Avda. Complutense, 22, 28040 Madrid, Spain

Abstract

The studies about the behaviour of ^{79}Se and ^{93}Zr allow identifying the PUREX process streams in which these radionuclides remain. In this way, in further investigations, other specific separation techniques could be applied in order to get targets pure enough for their possible transmutation. The studies showed that the extraction of Se decreases when the acidity of the aqueous phase increases from 0.5 M to 8.0 M, obtaining D values from 1.1E-2 to 3.4E-4 respectively and the uranium concentration has not influence in the Se extraction up to 130 g/L. In the case of Zr, its distribution coefficent value increases when the acidity of the medium increases from 1.96E-2 to 3.84E0 and 3.1 M to 8.0 M respectively, but the study about the influence of the uranium concentration in the Zr extraction showed that the Zr distribution coefficient decreases down to 1.0E-2 when the organic phase is 100% saturated in uranium (130 g/L). Then it can be concluded that ^{79}Se and ^{93}Zr remain in the raffinate of the first step of PUREX process.

1. Introduction

The study of the behaviour of some fission products such as ^{79}Se, ^{93}Zr, ^{107}Pd and ^{126}Sn about their possible liquid-liquid extraction, together with uranium and plutonium, by the tributhyl phosphate (TBP) in the main steps of the process for U and Pu separation and purification in the irradiated nuclear fuel reprocessing (PUREX process), is considered one of the main lines of the project *Long-lived Radionuclides Separation by Hydrometallurgic Processes* developed within the framework of CIEMAT-ENRESA agreement.

The main steps of the PUREX process consist on a jointly separation of U and Pu from the dissolution of a spent fuel (Figure 1), which are separated in a later step, by consecutive re-extraction processes, being necessary to reduce the oxidation state of Pu(IV) to Pu(III) and to use a weak acidic medium for U re-extraction. Then, both elements are purified independently by liquid-liquid extraction processes.

The aim of this paper is to show the studies carried out about the behaviour of ^{79}Se and ^{93}Zr, in order to identify the PUREX process streams in which these radionuclides remain. In this way, in further investigations, other specific separation techniques could be applied in order to get targets pure enough for their possible transmutation.

Figure 1. **Simplified flow diagram of PUREX process**

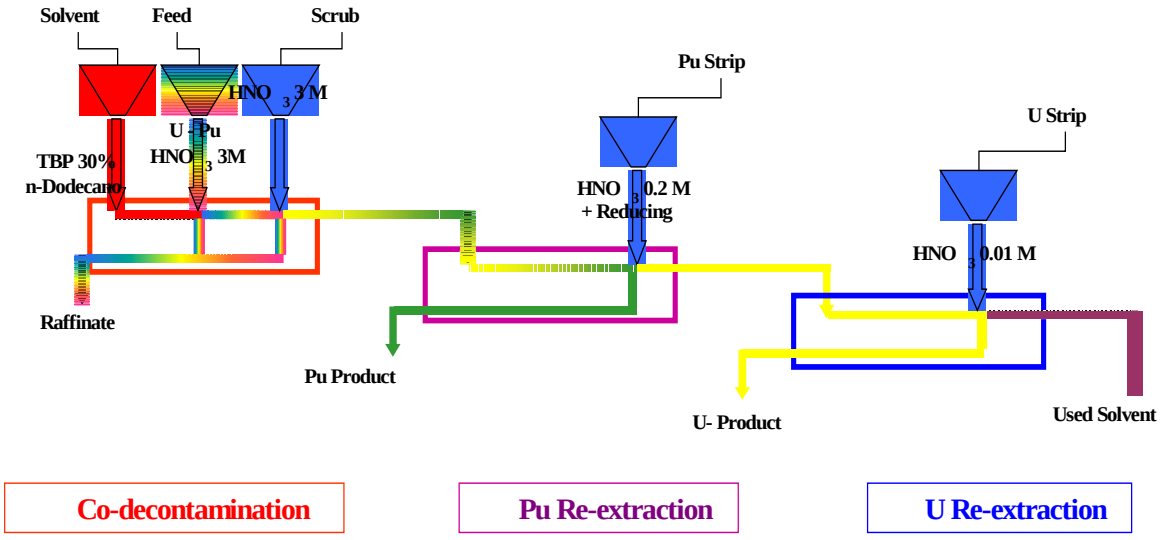

2. Experimental

2.1 Reagents

- Analytical grade TBP, n-dodecane, nitric acid, $Na_2SeO_3 \cdot 5H_2O$ and $ZrOCl_2 \cdot 8H_2O$.
- Uranium of nuclear purity prepared from nitric digestion of UO_3.
- Beta-gamma tracers of ^{75}Se and ^{95}Zr (Amersham UK).

2.2 Chemical speciation

The oxidation states of selenium in nitric acid medium, considering the conditions in which the irradiated nuclear fuel is dissolved in the first step of PUREX process, can be (IV) and (VI), although Se(IV) is the most stable oxidation state in aqueous solution, and its chemical form in acid nitric medium is H_2SeO_3 [1].

The chemical form of zirconium is difficult to evaluate due to its strong tendency to hydrolyse. Depending on the medium acidity, zirconium forms complexes and generates a great variety of colloid species. The tetra-positive ion is considered the dominant zirconium specie in the first step of PUREX process, where the nitric acid concentration is high [2].

Depending on the acidity of the medium, zirconium can be extracted by TBP-dodecane in the form of di-, tri- or tetra nitrate complex [3-6]: $Zr(OH)_2(NO_3)_2(TBP)_2$, $ZrOH(NO_3)_3(TBP)_2$, $Zr(NO_3)_4(TBP)_2$.

2.3 Reference irradiated nuclear fuel

To calculate the concentration of Se and Zr present in an irradiated nuclear fuel, a burnt up of 40 000 MWd/tU, 3.5% enrichment and a cooling time of 5 years were considered. This reference fuel element is the same used by ENRESA in the calculation and assumptions concerning the project *Spent Fuel Characterisation and Behaviour under Relevant Repository Conditions* [7].

2.4 Experimental conditions and equilibrium diagrams

The studies were carried out considering a mass concentration of 67.5 g Se/tU and 4 284 g Zr/tU. The uranium concentrations considered were 25, 50, 100, 150, 200, 250 and 300 g/L.

Se(IV) and Zr(IV) equilibrium diagrams were obtained in the following conditions, which are those of the first extraction and scrubbing step of the PUREX process [8,9]:

- HNO_3 concentration: 3, 4 and 5 M.
- TBP in dodecane concentration: 20, 25 and 30% (v/v).
- Phase ratios (Or/Aq): 1, 2 and 3.
- Se(IV) concentration: 1.70, 3.40, 6.80, 10.2, 13.6, 17.0 and 20.4 mg/L
- Zr(IV) concentration: 0.11, 0.22, 0.43, 0.64, 0.86, 1.07 and 1.28 g/L.

The stable Se(IV) and the tracer ^{75}Se were prepared in the same chemical form SeO_3^{2-}. This specie was obtained by flow back boiling $Na_2SeO_3 \cdot 5H_2O$ and ^{75}Se in nitric acid 3, 4 and 5 M.

The stable Zr(IV) as ZrO_2Cl_2 and the tracer ^{95}Zr were treated successively with HNO_3 18 M to obtain the specie $ZrO_2(NO_3)_2$.

The influence of the uranium concentration was studied considering those nitric acid concentrations in which the extraction of both, Se(IV) and Zr(IV), was maximum. The uranium concentrations tested were ranged from 25 g/L to 300 g/L.

Plutonium was simulated with the non active chemically analogous element Ce(IV) being the total mass 2 861 gCe/tU.

Se(IV) and Zr(IV) were tested independently and the equilibria were carried out with TBP-dodecane as organic phase. The equilibria between nitric and TBP phases were reached by 30 minutes of mechanical shaking at 950 u/min and the separation was performed after 60 minutes of decantation time. ^{75}Se, ^{95}Zr, free $[H^+]$ and uranium determinations were carried out in both phases.

Results are detailed in Figures 2 to 7 and Tables 1 to 4.

2.5 Analytical procedures

- Determination of Se concentration: it is performed by gamma spectrometry using the net peak area at 136 keV line of ^{75}Se.
- Determination of Zr concentration: it is performed by gamma spectrometry using the net peak area at 724 keV line of ^{95}Zr.
- Determination of free $[H^+]$: the cations present in the sample are complexed or precipitated by an excess of oxalic/oxalate buffer at pH 7.0. The solution is potentiometric titrated with KOH 0.1 M until pH 7.0.
- Determination of U concentration (Method I): gravimetry as U_3O_8.
- Determination of U concentration (Method II): it is performed by gamma spectrometry using the net peak area at 186 keV line of ^{235}U.

3. Results and discussion

3.1 Extraction of Se(IV)

The extraction equilibrium diagrams of Se(IV) show the typical isothermal curves that are generally obtained in these kind of studies (Figure 2). For all TBP concentrations studied, the extraction of Se(IV) decreases when the acidity of the aqueous phase increases. The maximum value of the distribution coefficient (D), obtained for the lower acid media in the steady state (1.83 M) is 4.5E-3 (Table 1), which indicates the low Se(IV) extraction in these conditions.

Figure 2. **Isothermal equilibrium curves of Se(IV) with different HNO_3(M) and TBP-dodecane concentrations. Or/Aq phase ratio 1**

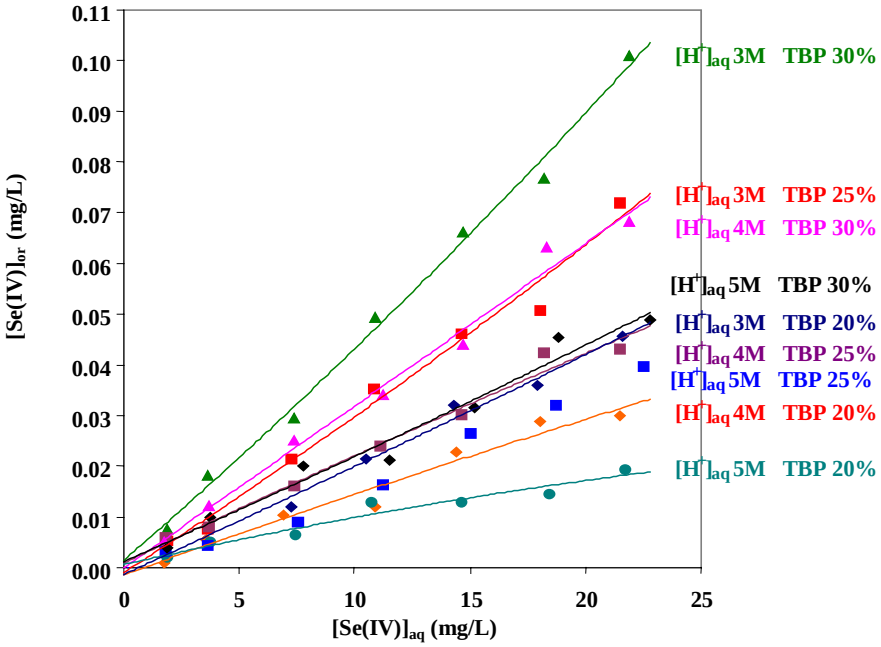

Table 1. **Distribution coefficients of Se(IV) by TBP 30% in dodecane. Initial Se(IV) concentration 20.4 mg/L.**

H^+ (M) Aq. phase	Ratio Or/Aq	Steady state					
		H^+ (M) Aq. phase	U (g/L) Aq. phase	U (g/L) Or.phase	Se(IV) (mg/L) Aq. phase	Se(IV) (mg/L) Or. phase	Distribution coefficient (D)
2.99	3	1.83	0	0	21.9	0.0977	4.46 E-3
2.99	2	2.12	0	0	22.0	0.0882	4.04 E-3
2.99	1	2.49	0	0	21.3	0.0733	3.44 E-3
3.90	3	2.53	0	0	21.9	0.0683	3.12 E-3
3.90	2	2.87	0	0	21.5	0.0563	2.62 E-3
5.27	3	3.43	0	0	22.8	0.0488	2.14 E-3
3.90	1	3.46	0	0	20.8	0.0450	2.16 E-3
5.27	2	3.90	0	0	22.0	0.0376	1.71 E-3
5.27	1	4.21	0	0	22.4	0.0296	1.32 E-3
3.02	3	1.93	< 0.5	9	21.9	0.204	9.32 E-3
3.00	3	1.92	1	17	21.6	0.348	1.61 E-2
2.94	3	2.00	1	36	21.5	0.453	2.11 E-2
3.14	3	2.24	1	52	22.4	0.178	7.96 E-3
3.03	3	2.30	2	68	22.8	0.105	4.60 E-3
3.07	3	2.47	6	83	23.4	0.0941	4.02 E-3
3.10	3	2.55	35	125	21.7	0.0621	2.86 E-3
3.09	3	2.60	170	138	22.2	0.0511	2.30 E-3

The influence of uranium and plutonium concentration in the distribution coefficient of Se(IV), was tested in the conditions in which the Se extraction is maximum (TBP 30% and HNO_3 3 M).

The obtained results (Table 1 and Figure 3) show that uranium concentration has not influence in the extraction of Se(IV), because the D value increment is not significant. For this, it can be established that Se(IV) is not extracted in the first U and Pu co-extraction step of the PUREX process.

Figure 3. **Influence of U concentration (g/L) on distribution coefficient of Se(IV), TBP-dodecano 30% HNO_3 5 M**

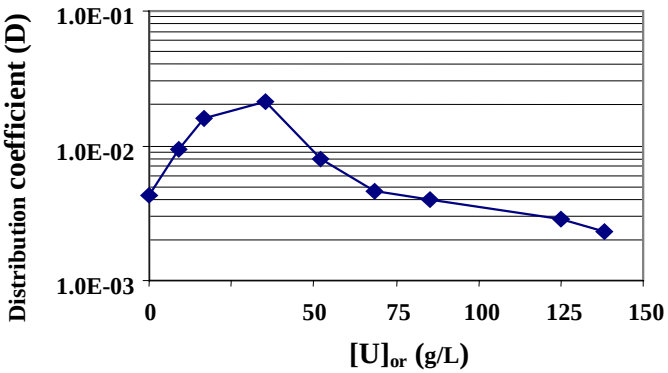

In order to complete the study about the influence of the aqueous nitric acid concentration in the Se(IV) extraction, samples with acid nitric concentrations between 0.5 M and 3 M and between 6 M and 8 M were analysed considering the maximum extraction conditions (TBP 30% and Se(IV) concentration 20.4 mg/L).

Figure 4. **Influence of HNO_3 concentration (M) on extraction coefficient of Se(IV) by TBP-dodecane 30%**

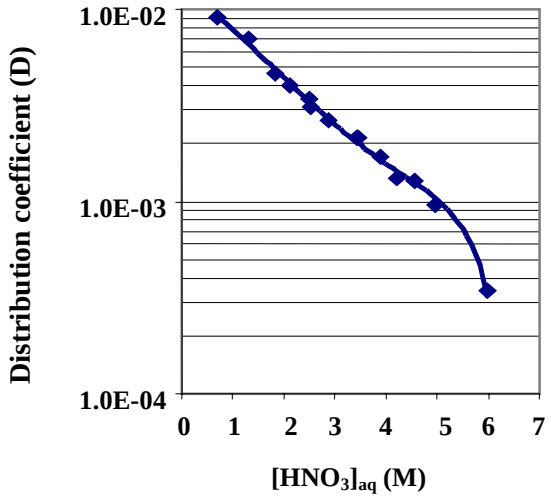

Table 2 and Figure 4 show that the tendency of the Se(IV) distribution coefficient is the same observed before, nevertheless the maximum D value obtained is 1.0E-2 that means Se(IV) is not extracted by TBP, so it can be concluded that ^{79}Se remains in the raffinate of the first step of PUREX process.

Table 2. **Influence of aqueous acid nitric concentration less than 3 M and higher than 5 M, in the distribution coefficient of Se(IV) by TBP 30% in dodecane. Initial Se(IV) concentration 20.4 mg/L.**

H^+ (M) Aq. phase	Ratio Or/Aq	Steady state			
		H^+ (M) Aq. phase	Se(IV) (mg/L) Aq. phase	Se(IV) (mg/L) Or. phase	Distribution coefficient (D)
0.524	3	0.39	21.0	0.223	1.06 E-2
1.06	3	0.69	20.9	0.191	9.12 E-3
2.13	3	1.31	21.4	0.149	6.98 E-3
6.17	3	4.56	22.3	0.0285	1.28 E-3
7.22	3	4.97	23.6	0.0228	9.67 E-4
8.20	3	5.99	22.9	0.0078	3.43 E-4

3.2 Extraction of Zr(IV)

The extraction equilibrium diagrams of Zr(IV) show the typical isothermal curves obtained in this kind of studies (Figure 5). Although the maximum extraction is obtained when the aqueous nitric acid and TBP concentrations are high, Zr(IV) is not extracted by TBP in a significant quantity because the maximum distribution coefficient value is 0.55 (Table 3) obtained for an acidity in the steady state of 4.7 M.

Figure 5. **Isothermal equilibrium curves of Zr(IV) with different HNO_3 (M) concentration and TBP-dodecane % concentrations**

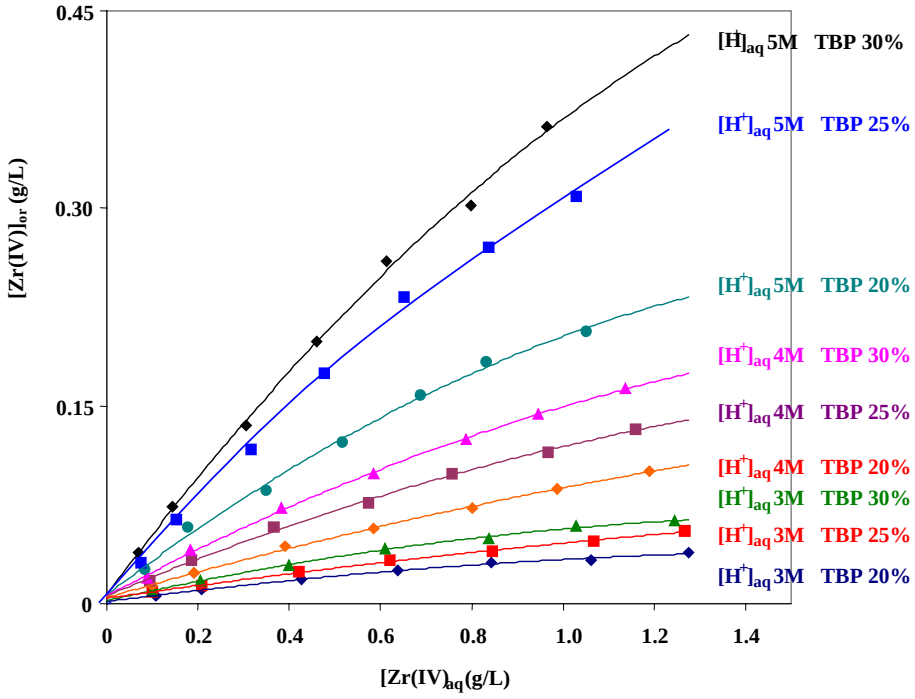

The influence of uranium and plutonium concentration in the distribution coefficient of Zr(IV) was tested in the conditions in which the extraction is maximum, TBP 30% and HNO_3 5 M.

The obtained results (Table 3 and Figure 6) show that when uranium concentration increases the Zr(IV) extraction decreases. The value of the distribution coefficient is very low (0.01) when the organic phase is 100% saturated with uranium (130 g/L). This effect shows that Zr(IV) is not extracted in the first cycle of co-extraction of U and Pu in the PUREX process.

Figure 6. **Influence of U (g/L) concentration on distribution coefficient of Zr(IV), TBP-dodecane 30%, HNO_3 5 M**

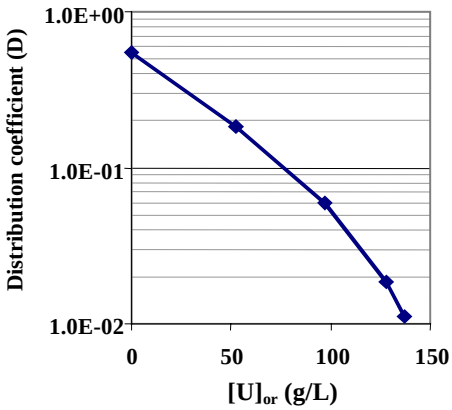

Due to the extraction of Zr(IV) by TBP increases as the nitric acid concentration increases (Figure 5), it is necessary to study the behaviour of Zr(IV) when the nitric acid concentration, in the aqueous phase is higher (from 5 M to 8 M) than the range considered in the first studies and within the maximum extraction conditions TBP 30% and Zr(IV) concentration 1.28 g/L.

Table 3. **Distribution coefficient of Zr(IV) by TBP 30% in dodecane. Initial Zr(IV) concentration 1.28 g/L**

H^+ (M) Aq. phase	Ratio Or/Aq	Steady state					
		H^+ M Aq. phase	U g/L Aq. phase	U g/L Or. phase	Zr(IV) g/L Aq. phase	Zr(IV) g/L Or. phase	Distribution coefficient (D)
3.08	3	1.86	0	0	1.31	0.0256	0.0196
3.08	2	2.13	0	0	1.29	0.0395	0.0307
3.08	1	2.49	0	0	1.25	0.0626	0.0203
4.07	3	2.55	0	0	1.14	0.0580	0.0510
4.07	2	2.92	0	0	1.16	0.0951	0.0823
5.06	3	3.20	0	0	0.993	0.119	0.120
4.07	1	3.48	0	0	1.14	0.163	0.144
5.06	2	3.70	0	0	0.935	0.192	0.205
5.06	1	4.39	0	0	0.966	0.362	0.375
5.50	1	4.70	0	0	0.827	0.452	0.547
4.89	1	4.68	< 0.1	52	1.12	0.206	0.183
4.97	1	4.82	< 0.1	97	1.26	0.0762	0.0605
4.88	1	4.88	23	128	1.34	0.0248	0.0185
4.91	1	4.88	76	135	1.34	0.0159	0.0119
4.99	1	4.90	118	138	1.33	0.0150	0.0113
4.89	1	4.90	168	137	1.36	0.0140	0.0103

Figure 7. **Influence of HNO_3 concentration (M) on distribution coefficient of Zr(IV) by TBP-dodecane 30%**

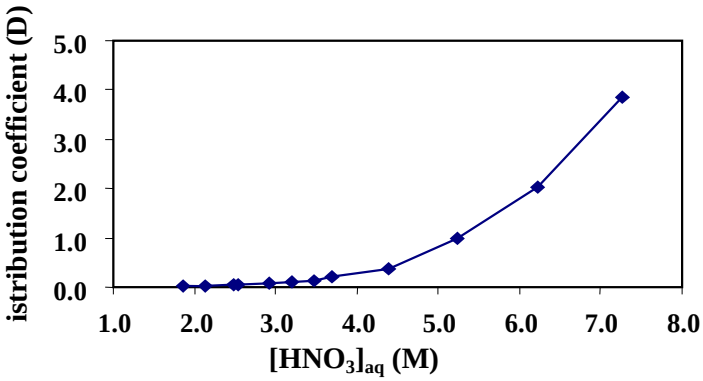

Table 4. **Influence of nitric acid concentration higher than 5 M on the distribution coefficient of Zr(IV) by TBP 30% in dodecane. Initial Zr(IV) concentration 1.28 g/L.**

H^+ (M) Aq. phase	Ratio Or/Aq	Steady state			
		H^+ (M) Aq. phase	Zr(IV) (g/L) Aq. phase	Zr(IV) (g/L) Or. phase	Distribution coefficient (D)
5.50	1	4.70	0.827	0.452	0.547
6.10	1	5.24	0.641	0.635	0.990
7.03	1	6.22	0.421	0.854	2.030
7.95	1	7.26	0.259	0.994	3.840

Results from Table 4 and Figure 7 show that the distribution coefficient values of Zr(IV) increase when the HNO_3 concentration increases, being the distribution coefficient higher than 1.0 for HNO_3 concentration higher than 6 M and close to 4.0 for acid concentrations of 8 M. This behaviour could be useful for a possible separation of ^{93}Zr from the raffinate of the first cycle of PUREX process, in which it has been demonstrated that Zr remains totally.

REFERENCES

[1] I.I. Nazarenko, A.M. Yermakov, *Analytical Chemistry of Selenium and Tellurium*, Analytical Chemistry of the Elements Series, 1971, Russian Academy of Sciences Publ., 1-32.

[2] W.B. Blumenthal, *The Chemical Behaviour of Zirconium*, 1958, Van Nostrand, Princenton N.J.

[3] G.F. Egorov, *Solvates of Zirconium and Hafnium Nitrates with TBP*, Russ. J. Inorg. Chem., 1960, 5, 503-505.

[4] A.E. Levitt, H. Freund, *Extraction of Zirconium by TBP*, J. Am. Chem. Soc., 1956, 78(8), 1545-1549.

[5] O.A. Sineergibrova, G.A. Yagodin, *Zirconium-hafnium Separation*, 1966, At. Energy Rev., 4, 93-99.

[6] A.S. Solovkin, *Thermodynamics of the Extraction of Zirconium, Present in the Monomeric State, From HNO_3 Solutions by TBP*, Russ. J. Inorg. Chem., 1970, 15, 983-984.

[7] ENRESA-2000, *Elemento Combustible de Referencia Irradiado: Inventario Másico y Radiactivo, Potencia Térmica Residual, Espectro Fotónico e Inventario Radiotóxico*, 1999 Clave 49-1PP-L-02-02.

[8] Y. Koma, T. Koyama, Y. Tomaka, *Recovery of Minor Actinides in Spent Fuel Reprocessing Based on PUREX Process*, RECOD'98, Niza, 1998, I, 409-416.

[9] O. Courson, R. Malmbeck *et al*., *Separation of Minor Actinides from Genuine HLLW Using the Diamex Process*, 5th International Information Exchange Meeting, Mol, 1998, EUR 18898 EN, OECD/NEA (Nuclear Energy Agency), Paris, France, 1999.

SOLUBILIZATION STUDIES OF RARE EARTH OXIDES AND OXOHALIDES. APPLICATION OF ELECTROCHEMICAL TECHNIQUES IN PYROCHEMICAL PROCESSES

C. Caravaca, P. Díaz Arocas, J.A. Serrano, C. González
CIEMAT, Dpto. de Fisión Nuclear, Avda. Complutense, 22, Madrid 28040, Spain
E-mail: c.caravaca@ciemat.es

R. Bermejo, M. Vega, A. Martínez and Y. Castrillejo
Universidad de Valladolid, Dpto Química Analítica, F. de Ciencias,
Prado de la Magdalena s/n, 47005 Valladolid, Spain.
E-mail: ycastril@qa.uva.es

Abstract

Chemical and electrochemical properties of rare earths (La, Ce, Pr and Y) chloride solutions in the eutectic LiCl-KCl and the equimolar $CaCl_2$-NaCl mixture were studied at 450 and 550^0C respectively.

The stability of the oxidation states of rare-earths and the standard potential of the different redox couples have been determined. The solubility product of oxides and oxychlorides were calculated, the differences observed on pKs values between the two molten media demonstrate the different oxoacidic properties of both molten baths. All these data have been summarised in E-pO^{2-} diagrams which displays the stability domains of rare earth compounds on each melt.

Gaseous HCl was used as chlorinating agent during the solubilization tests of the corresponding rare earth oxides and oxychlorides, efficiencies close to 100%.

The electrochemical behaviour of rare earth solutions has been studied at W and Mo electrodes using different electochemical techniques, observing that Me electrodeposition could be complicated by alkaline co-deposition (Li or Na). Mass transport towards the electrode is a simple diffusion process, and the diffusion coefficients of Me(III) were obtained. In LiCl-KCl, nucleation and crystal growth of the rare earth metal seems to be the controlling step in most cases, while in $CaCl_2$-NaCl this phenomenon has not been observed.

1. Introduction

The long-term radiological hazard of spent nuclear fuel is determined by the transuranium elements (TRU: Pu, Am, Cm, Np) and some long-lived fission products (LLFP: Cs, I, Tc). If these elements could be separated efficiently from the spent fuel and be transformed into short-lived or stable ones, a significant positive on the overall performance repository will be achieved [1].

Over the last years, a renewed interest on pyrochemical separation processes in molten salt media has been shown mainly due to the progress in the assessment of new concepts for transmutation and the corresponding fuel cycles [2]. Pyrochemical processes are considered to have potential advantages over aqueous processes to reduce the inventory of actinides and long lived fission products in the nuclear wastes. In order to assess its feasibility, several processes have been developed for the recovery of actinides from spent metallic, nitride, oxide nuclear fuels, and high level radioactive liquid wastes [3].

Some of the main advantages of the pyrometallurgical process are that the purity of the product is less stringent, the recovery of minor actinides takes place simultaneously with plutonium due to the thermodynamic properties in molten salt. The recovery of minor actinides allow the reduction of TRU. On the other hand, the radiation stability of molten salt enables to process spent fuels of high radioactivity without increasing the secondary waste, and since molten salt does not act as neutron moderator comparatively higher amount of fissile material can be handled in the processes equipment than in the aqueous processes [4].

Since the separation behaviour of actinides and rare-earths is essential for designing the pyrochemical processes, much effort has been made to study actinide and rare-earth chemistry in molten salt media in order to have a reliable data base [3]. As a part of a wider UE project that is focused on separation of actinides from LLFP from oxide nuclear fuels, the present work presents a study of the chemical and electrochemical properties of several rare-earths in two different molten chloride baths.

Separation prediction can be made from thermodynamic data by means of the so called generalised Pourbaix type diagrams (GPTD), E-pO^2, for rare earth (i.e. La, Ce, Pr and Y)-O compounds and the chlorinating gaseous mixtures in two molten chloride mixtures of different intrinsic acidities, the LiCl-KCl eutectic melt and the $CaCl_2$-NaCl equimolar mixture, which enables to propose the main lines for the pyrochemical separation process. Thermodynamic data of metal oxides are often available in the literature but unfortunately, in most cases, data for most of the pure metal oxychlorides are not available. Therefore, the stability of these species has to be experimentally determined by using specific tools such as the yttria-stabilized zirconia membrane electrode (*ysze*).

Electrochemical techniques provide an efficient tool to investigate the reaction mechanisms. The establishment of modern electrochemical technologies requires early engineering evaluation of the cell behaviour with reliable procedures. To reach a better view of the feasibility of the process, the kinetic parameters of the reaction steps are measured from transient techniques taking into account the diffusion's contribution of electroactive species, electron transfer, kinetics and additionally adsorption or crystallisation, the last one generally is controlled by the rate of nucleus formation and the diffusion of active species.

2. Experiment details

Cyclic voltammetry and other pulse techniques were performed. The working electrodes (WE) used were tungsten or molybdenum wires of 1mm diameter, as counter electrode tungsten was used. The active surface area of the WE was determined by measuring the depth of immersion.

The reference electrode consisted of a silver wire (1 mm diameter) dipped into a silver chloride solution (0.75 $molKg^{-1}$) in the $CaCl_2$-NaCl or LiCl-KCl molten mixture contained in a quartz tube. Potentials were measured by reference to the AgCl/Ag couple.

The pO^{2-} indicator electrode used is a tube of yttria-stabilised zirconia, filled with molten $CaCl_2$-NaCl or LiCl-KCl and oxide and silver ions (3×10^{-2} and 0.75 $molkg^{-1}$ respectively) in this mixture a silver wire was also immersed (inner reference Ag^+/Ag).

The chloride mixtures $CaCl_2$-NaCl or LiCl-KCl (analytical-grade) were melted under vacuum, next raised to atmospheric pressure using dry argon, and then it was purified by bubbling HCl through the melt for at least 30 minutes, and then kept under argon atmosphere [5-7]. Working temperature was measured by a thermocouple introduced into the melt. Salt handling was carried out in a glove box under argon atmosphere.

Solutions of the electroactive species was prepared by direct addition of $MeCl_3$. In order to remove any traces of oxide ions, the solutions were purified by gaseous HCl bubbling.

2.1 pK_s determinations

pKs determinations were performed using a *ysze* electrode placed into the melt. A known amount of metal ion introduced as chloride was potentiometrically titrated either with Na_2CO_3 or BaO. Continuous stirring with dried argon was required.

3. Results and discussion

3.1 Determination of the stable oxidation states of rare earths

The electrochemical properties of dilute solutions of rare earth ions (Ce(III), La(III), Pr(III) and Y(III)) in the equimolar $CaCl_2$-NaCl and eutectic LiCl-KCl, at 550 and 450^oC respectively, were studied.

Figure 1 shows voltammograms obtained with a solution of $CeCl_3$ in the eutectic LiCl-KCl melt using a tungsten electrode. The process is characterised by one cathodic peak well defined, associated with the corresponding sharp re-oxidation peak, (anodic dissolution), which is characteristic of the formation of a product that remains adhered to the electrode. This fact has been confirmed by examination of the voltammograms, the ratio of the anodic to the cathodic current was higher than unity, the ratio between the total anodic to cathodic charge was close to unity and independent of the scan rate (Figure 2). In the anodic region, there was not observed the electrochemical system Ce(IV)/Ce(III), in none of the melts, which indicate that the standard potential of that system is out the range accessible in these melts, and that Ce(IV) is a powerful oxidizing agent which oxidizes the chloride ions of the melt according to the reaction:

$$Ce(IV) + Cl^- \leftrightarrow Ce(III) + 1/2\ Cl_2\ (g) \qquad (1)$$

The voltammograms obtained for other rare earth trichlorides solutions,in both chloride melts, behaved in a similar way except for a positive or negative shift of the peak potential value compared to that of the $CeCl_3$. Moreover, it has been observed that the peak potential values obtained in the melt $CaCl_2$-NaCl are slightly less cathodic than those obtained in the eutectic LiCl-KCl.

Figure 1. **Cyclic voltammograms of LiCl-KCl with $CeCl_3$ ($1.57.10^{-4}$ mol/cm^3), W_E: tungsten 0.28 cm^2**

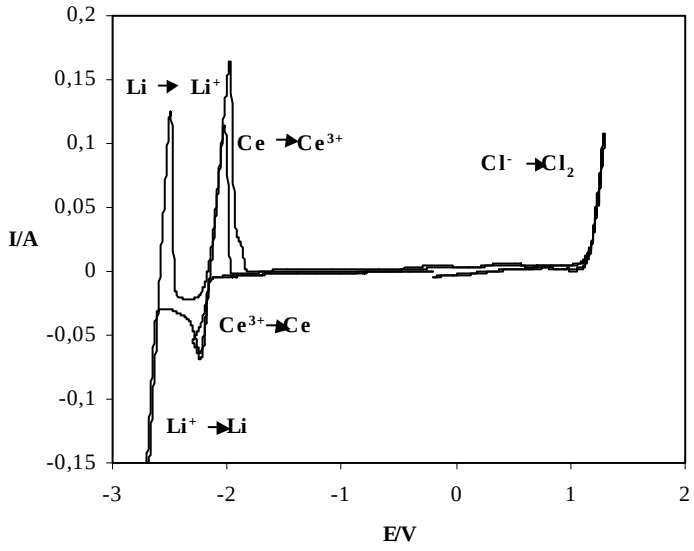

Figure 2 (a). **Voltammogram that proves the formation of a solid product at the tungsten surface. Reduction step Me(III)+3e ⇔Me and the subsequent anodic dissolution of the deposit**

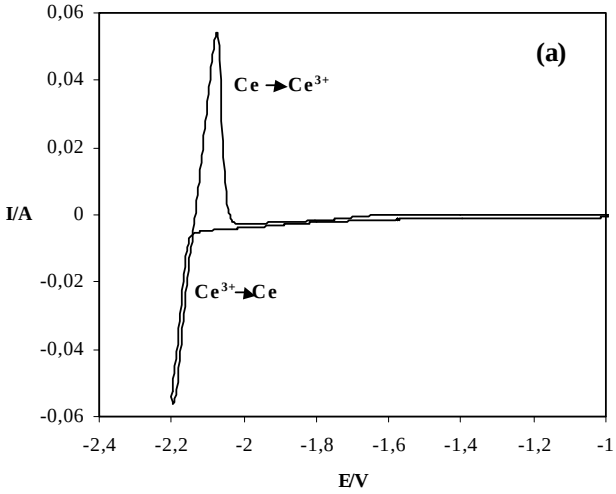

Figure 2 (b). **Comparison between the cathodic and anodic charge for the deposition and subsequent reoxidation of solid cerium**

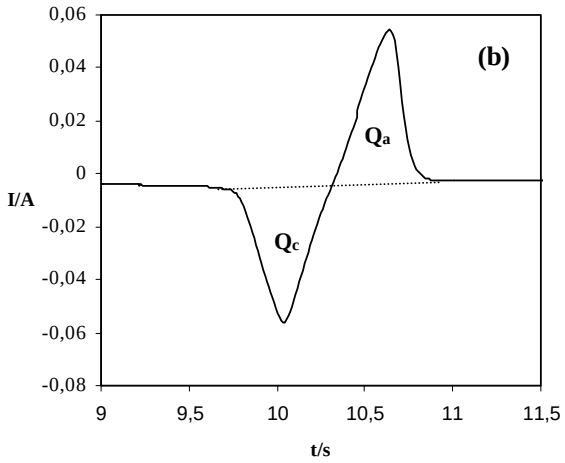

Square wave voltammetry (SWV) to study the stable oxidation states of rare earths in both melts was used. According to Baker *et al.* [8] and Osteryoung *et al*. [9] the width of the half-peak, $W_{1/2}$, depends on the number of electrons exchanged and on the temperature as follows:

$$W_{1/2} = 3.52\frac{RT}{nF} \qquad (2)$$

The n-values obtained with all the $MeCl_3$ solutions were close to 3.

Similar results were obtained by chronopotentiometry. This type of transients show the existence of a potential plateau in the range –2,20 V (v.s. Ag^+/Ag). After this plateau a rapid decrease was observed, and then, the electrode potential reaches a limiting value corresponding to the deposition of alkaline metals (Figure 3).

The reduction of rare earth trichlorides (La(III), Ce(III), Pr(III) and Y(III)) to metal takes place in a single step, according to the reaction:

$$Me(III) + 3e \leftrightarrow Me(s) \qquad (3)$$

Figure 3. **Chronopotentiograms for the reaction $Pr^{3+} + 3e \leftrightarrow Pr$ in LiCl-KCl**

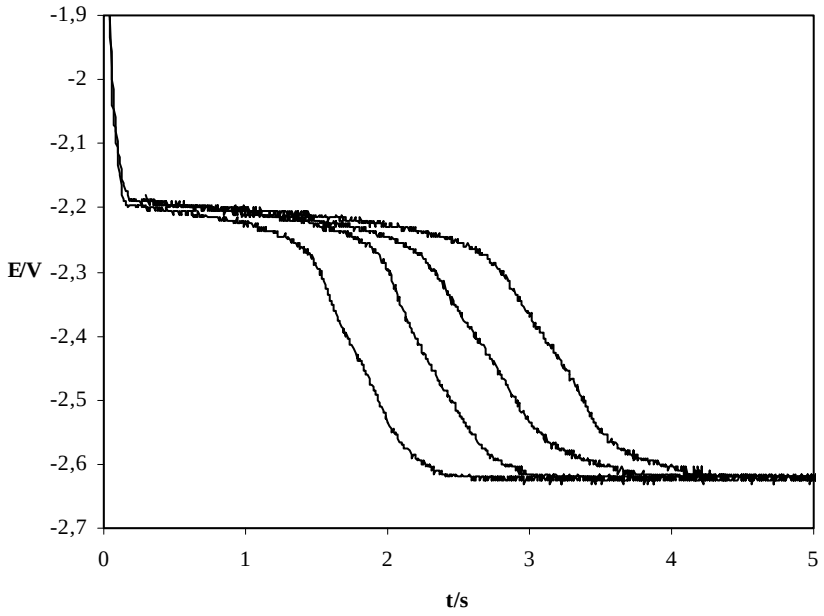

3.2 Standard potential of Me(III)/Me(0), and activity coefficient $\gamma(MeCl_3)$ determination

The standard potential of the redox couples Me(III)/Me was determined by measuring the equilibrium potential of a tungsten wire covered with an electrodeposit of Me(0), obtained by coulometry at a constant potential value, avoiding any alkaline deposition.

For each rare earth the e.m.f values were measured for several metal chloride concentrations. Based on these measurements the variations of the e.m.f. is given by the Nernst equation. The plots of the e.m.f. versus the logarithm of the Me(III) concentration were linear with slopes in agreement with the theoretical values for a three-electron process. The standard potentials were deduced from linear extrapolation of the plots at a $MeCl_3$ concentration equal to 1 mol/kg, (see Table 1). The apparent standard potentials are very close, and in the order:

- Eutectic LiCl-KCl: La > Ce > Y, Pr.
- Equimolar $CaCl_2$-NaCl: La > Ce > Pr.

According to Equation (4) the standard potentials can also be deduced from the peak potential values of the voltammetric reduction of Me(III) [10].

$$E_p = E^o + 2.3\frac{RT}{nF}\log C_o - 0.849\frac{RT}{nF} \qquad (4)$$

This equation is valid for conditions where the electrochemical reaction is diffusion controlled. The E^0 values derived, (see Table 1, c.v. values), were several mV more negative than those obtained by e.m.f. measurements. This is probably due to the quasi-reversible behaviour of the electrochemical system, and/or to the influence of nucleation and crystal growth phenomena, since Equation (4) does not take into account any of those phenomena.

Activity coefficients of $MeCl_3$ in the melts, γ_{MeCl3} which take into account the free enthalpy of formation of $MeCl_3$(s) and of solvated $MeCl_3$(dissolved) were calculated by the ΔE corresponding to the reaction:

$$Me + 3/2\ Cl_2 \leftrightarrow MeCl_3\ (dissolved) \qquad (5)$$

and related with the ΔE^* of the same reaction between pure compounds, by means of the equation:

$$\log \gamma_{MeCl3} = (\Delta E^* - \Delta E)3F/2.3RT \qquad (6)$$

ΔE^* was derived from the literature [11] and ΔE from previously recorded experimental data. The values obtained are given in Table 1.

Table 1. **Standard potential values and activity coefficient of some rare-earths chlorides in LiCl-KCl and $CaCl_2$-NaCl**

	LiCl-KCl			**$CaCl_2$-NaCl**		
Redox couple	Standard Potential/V Molality scale	ΔE^*/V	log γ_{MCl3}	Standard Potential/V Molality sacale	ΔE^*/V	log γ_{MCl3}
Ce(III)/Ce	*e.m.f.*-3.155 *c.v.* .-3.201	3.034	-2.53	*e.m.f.*-3.034 *c.v.* .-3.074	2.949	-1.56
La(III)/La	*e.m.f.*-3.160 *c.v.* -3.254	3.100	-1.26	*e.m.f.*-3.138 *c.v.*-3.174	3.023	-2.11
Pr(III)/Pr	*e.m.f.*-3.150* *c.v.* -2.985*	3.032	-2.47*	*e.m.f.*-3.020* *c.v.* –3.007*	2.952	-1.25*
Y(III)/Y	*e.m.f.*-3.152* *c.v.* –3.305	2.774	-7.91*	– *c.v.* –3.023*	2.698	–

* Preliminary results.

The activity coefficient of rare earth chlorides gives information about the complexation of the cations by the melt. The complexation power depends both on the nature of the cations of the molten salts and on the working temperature. In the melt $CaCl_2$-NaCl at 550°C, which is a more oxoacidic than the eutectic LiCl-KCl, the activity coefficients values obtained are higher than in LiCl-KCl, except for lanthanum. This corresponds to a lower complexation of the $MeCl_3$ by the chloride ions of the melt, which indicates more stable complex ions formation.

3.3 Stability of Me(III)-O compounds. pk_s determination

Identification of the rare earth oxides and oxohalides that are stable in both melts, can be accomplished by the theoretical analysis of the curves obtained by potentiometric titration [12,13]. The solubility of the oxides and oxyhalides can be determined theoretically from the analysis of the experimental titration curves.

Figure 4. **Potentiometric titrations of (a) 0.0797 mol kg^{-1} Pr(III) and (b) 0.1040 Y(III) solutions by O^{2-} ions added as solid Na_2CO_3.in the eutectic LiCl-KCl at 450°C.**

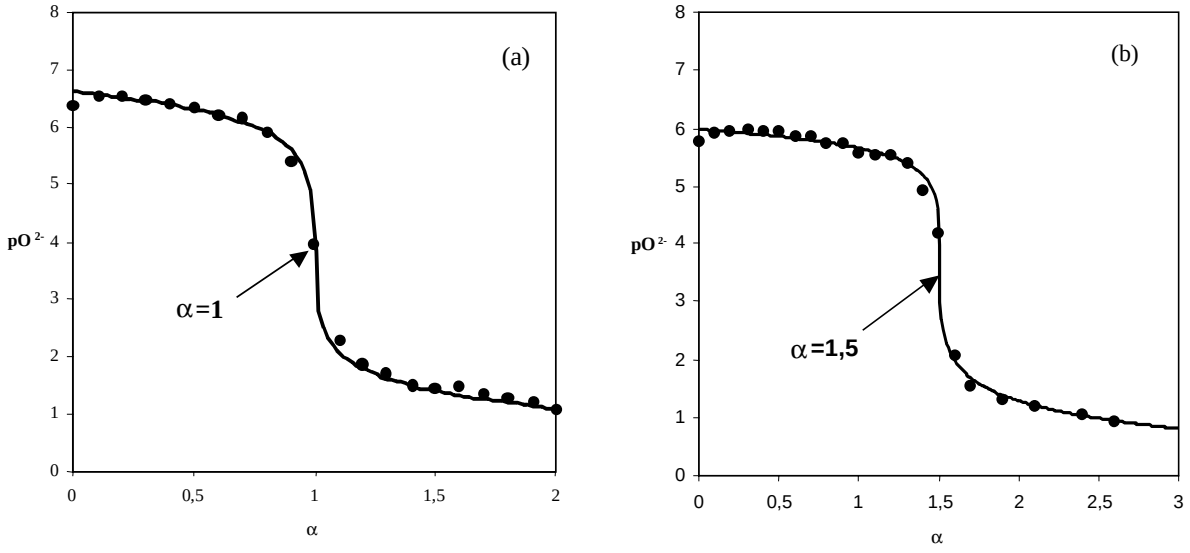

The rare-earth ions were precipitated with oxide (added as Na_2CO_3 or BaO), this reaction was monitored with an *ysze* [7,14-16]. A e.m.f. jump occurrs at the point corresponding to the stoichiometric precipitation of the corresponding oxide or oxohalide. Except for the YCl_3 all the experimental curves obtained with lanthanide ions exhibited similar habits to the one of Figure 4.a. The pO^{2-} values measured by the *ysze* (after calibration), show only one equivalent point for a stoichiometric ratio:

$$\alpha = \frac{\left[O^{2-}\right]_{added}}{[LnCl_3]initial} = 1.0 \qquad (7)$$

This indicates that the reaction is:

$$Ln^{3+} + O^{2-} + Cl^{-} \leftrightarrow LnOCl(s) \qquad (8)$$

For the YCl_3 solutions titrated in the eutectic LiCl-KCl by O^{2-} (Figure 4 (b)), only one equivalence point was observed for a stoichiometric ratio of α=1.5.

This value indicates that the reaction is in this case:

$$2Y^{3+} + 3O^{2-} \Leftrightarrow Y_2O_3\,(s) \qquad (9)$$

and it can be deduced that no oxychloride species were stable under the present experimental conditions. The LnOCl and Y_2O_3 formation was confirmed by XRD spectrometry analysis.

The theoretical equation corresponding to the titration curve can be elucidate from the mass balance and the solubility product of the reactions, according to the procedure previously described [7,14,15]. The solubility products of LnOCl and Y_2O_3, k_s, were determined by applying the Gauss-Newton non-linear least-squares method to the equation of the corresponding titration curves. The values obtained are shown in Table 2.

Table 2. **Solubility products, pk_s of the different oxychlorides and oxides**

Compounds	LiCl-KCl (450°C)	$CaCl_2$-NaCl (550°C)
CeOCl	7.45 ± 0.05	5.62 ± 0.07
LaOCl	7.00 ± 0.09	5.19 ± 0.05
PrOCl	7.45 ± 0.25	5.27
Y_2O_3	19.90 ± 0.22	–

3.4 Solubilization studies

With the solubility products of the Ln-O compounds and the equilibrium potentials of the different red-ox couples involved, it is possible to establish the potential-acidity diagram for the Ln-O species in both melts (Figure 5).

Figure 5. **Comparison of the potential-acidity diagram for the Ce-O compounds with the E-pO^{2-} diagram of the gaseous mixtures in the equimolar $CaCl_2$-NaCl mixture at 550ºC. MIXTURES: I: $Cl_2 + O_2$, II: $Cl_2 + C$, III: $Cl_2 + CO$, IV: $HCl + H_2O$, V: $HCl + H_2O + H_2$, VI: $HCl + H_2 + CO$**

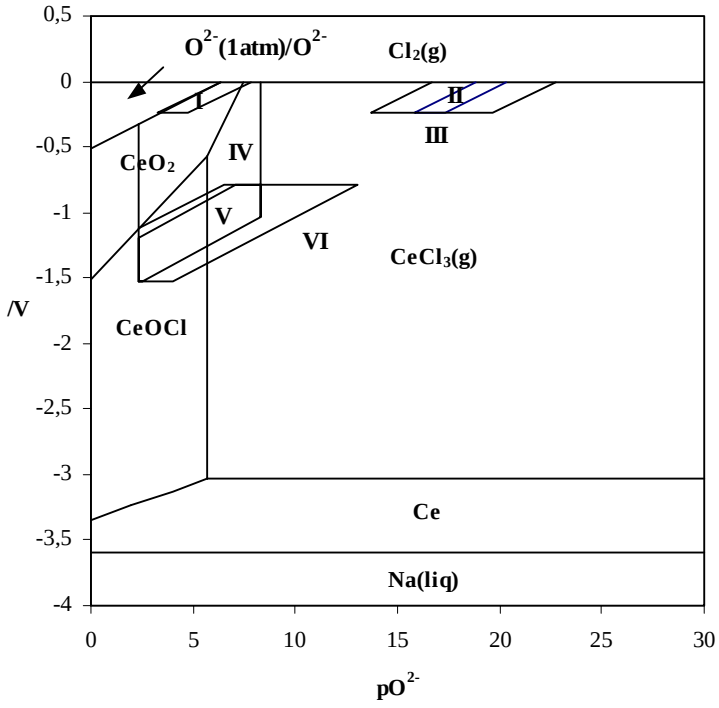

This type of diagrams gives the oxo-acidity and red-ox properties of the elements in the molten salt mixtures, being possible to predict electrochemical properties and some chemical reactions. The comparison of these diagrams to the those obtained for some gaseous mixtures in the same melt and temperature [6,14,15], allows to predict optimal chlorinating conditions for rare earth oxides and oxychlorides. It is observed in the Figure that all the LnOCl, CeO_2 and Y_2O_3 can be chlorinated by HCl.

Experimental solubilization tests were carried out: i) with samples of LnOCl generated *in situ*, and ii) samples of commercial La_2O_3, CeO_2, Pr_6O_{11} and Y_2O_3. As chlorinating agent HCl was used, and the reaction progress was followed by potentiometry with an *ysze*. After the dissolution an electrochemical spectra was recorded.

During the chlorination, the oxide ions are transformed into water by HCl, according with the following reactions:

$$2HCl + LnOCl \leftrightarrow LnCl_3(disolved) + H_2O \quad (10)$$

$$6HCl + Y_2O_3 \leftrightarrow 2YCl_3(disolved) + 3\ H_2O \quad (11)$$

For CeO_2 and Pr_6O_{11}, the chlorination could occur in two stages, in the first one it is formed the oxidizing Ce(IV) which reacts with the melt evolving $Cl_2(g)$ and dissolving $CeCl_3$, and the insoluble PrOCl respectively.

The concentration of the dissolved rare earths was determined *in situ* by titration of the final solution with sodium carbonate, showing efficiency values close to 100%.

3.5 Metal electrodeposition studies

The mechanism of electroreduction of rare-earth ions in the equimolar $CaCl_2$-NaCl and eutectic LiCl-KCl has been studied by electrochemical techniques. Previous experiments showed that refractory metals such as tungsten or molybdenum are suitable materials to use as electrodes in both melts. It is not possible to use glassy carbon due to the formation of Na-C or Li-C compounds [14].

The diffusion coefficient of the Me(III) ions could be calculated from the data obtained in the rare earth electrodeposition studies (Table 3).

Table 3. **Me(III) diffusion coefficients**

	LiCl-KCl (450ºC)		**$CaCl_2$-NaCl (550ºC)**	
	W	Mo	W	Mo
Ce(III)	1.0×10^{-5}	1.1×10^{-5}	9.2×10^{-6}	8.8×10^{-6}
La(III)	8.9×10^{-6}	8.4×10^{-6}	7.7×10^{-6}	7.8×10^{-6}
Pr(III)	9.4×10^{-6}	–	9.8×10^{-6}	–
Y(III)	1.5×10^{-5}	1.3×10^{-5}	1.3×10^{-5}	–

The diffusion coefficient values obtained in both media were similar. These results can be explained considering the opposite effect of the temperature and viscosity of the melt: The higher temperature in the case of the molten $CaCl_2$-NaCl mixture should produce an increase in the diffusion coefficient values, however, its higher viscosity leads to lower D values.

Chonoamperometric studies did not show evidence of nucleation phenomena in the equimolar $CaCl_2$-NaCl mixture under the experimental conditions tested. However, the I-t transients obtained in the eutectic LiCl-KCl have proved that nucleation of metallic lanthanum and yttrium plays a significant role in the overall electrodeposition process. Differences between the results obtained in both molten chlorides could be related to the differences on surface tension of the melts, which affect

the interactions Me-substrate and Me-substrate-melt. Information about nucleation kinetics was obtained applying a dimensionless method.

The efficiencies in the rare earth electrodeposition processes were calculated from double potential step measurements, for several potential impossed. The results show that alkaline metal co-deposition can interfere with the metal electrodeposition, complicating thus the process.

Acknowledgements

The authors would like to thank Francisco de la Rosa (Universidad de Valladolid) and Luis Gutierrez (CIEMAT) for the technical assistance and ENRESA (Spain) for the financial support (CIEMAT-ENRESA and CIEMAT-Universidad de Valladolid agreements).

REFERENCES

[1] H. Gruppelaar, J.L. Kloosterman and R.J.M. Konings, *Advanced Technologies for the Reduction on Nuclear Waste*, ECN report, 1998.

[2] OECD Nuclear Energy Agency, *Actinide and Fission Product Partitioning and Transmutation. Status and Assessment Report*, Paris, France, 1999.

[3] Y. Sakamura, T. Inoue, O. Shirai, T. Iwai, Y. Arai and Y. Suzuki, *Proceedings of Global'99*, Jackson Hole, Wyoming, USA, 1999.

[4] T. Koyama, K. Kinoshita, T. Inoue, M. Ougier, J.P. Glatz and L. Koch, *Workshop on Pyrochemical Separation OECD/NEA*, Work 3b-4, Avignon, France, March 2000.

[5] D. Ferry, Y. Castrillejo, G. Picard, *Acidity and Purification of the Molten Zinc Chloride (33.4 mol%)-sodium Chloride (66.6 mol%) Mixture*, Electrochim. Acta, 1989, 34(3), 313-316.

[6] F. Seón, *Tesis Doctoral de Estado*, París, 1981

[7] Y. Castrillejo, A.M. Martínez,, G.M. Haarberg, B. B•rresen, K.S. Osen and R. Tunold, *Oxoacidity Reactions in Equimolar Molten $CaCl_2$-NaCl Mixture at 550°C*, Electrochim. Acta, 1997, 42, 1489-1494.

[8] G.C. Baker, Anal. Chim. Acta, 1958, 18, 118.

[9] J. Osteryoung, J.J. O'Dea, *Determining Kinetic Parameters from Pulse Voltammetric Data*, Electroanal. Chem., 1986, 14, 209.

[10] A.J. Bard, L.R. Faulkner, *Electrochemical Methods*, J. Wiley New York, USA, 1980.

[11] J. Barin, O. Knacke, *Thermochemical Properties of Inorganic Substances*, Springer, Berlin, Germany, 1973.

[12] H. Lux, Z. Elektrochemi., (1948), 52, 220, (1949), 53, 41.

[13] H. Flood T. Förland and K. Motzfeld, *The Acidic and Basic Properties of Oxides,* Acta Chemica. Scandinavica., 1952, 6, 257.

[14] A.M. Martínez, Y. Castrillejo, E. Barrado, G.M. Haarberg and G Picard, *A Chemical and Electrochemical Study of Titanium Ions in the Molten Equimolar $CaCl_2$-NaCl Mixtures at 550°C,* J. Electroanal. Chem., 1998, 449, 67-80.

[15] Y. Castrillejo, M.R. Bermejo, A.M. Martínez, C. Abejón, S. Sánchez and G.S. Picard, *Study of the Electrochemical Behaviour of Indium Ions in the Molten Equimolar $Cacl_2$-NaCl Mixture at 550°C,* J. of Applied Electrochemistry, 29(1), 65-73, 1999.

CALIX[6]ARENES FUNCTIONALISED WITH MALONDIAMIDES AT THE UPPER RIM AS POSSIBLE EXTRACTANTS FOR LANTHANIDE AND ACTINIDE CATIONS

Marta Almaraz, Sagrario Esperanza, Oriol Magrans, Javier de Mendoza, Pilar Prados
Departamento de Química Orgánica, Facultad de Ciencias,
Universidad Autónoma de Madrid, Cantoblanco, 28029-Madrid, Spain

Abstract

Lipophilic malondiamides have been recently employed successfully as extractants for lanthanide and actinide cations from strongly acidic media. Many complexes between malondiamides and lanthanide-actinides cations have been studied by different techniques. For many of these complexes it has been observed that more than one malondiamide ligand participates in the complexation of each metallic cation. Incorporation of two or three malondiamide moieties into a calixarene platform would probably improve both extraction and selectivity with respect to the already tested malondiamides. According to CPK examination, a calix[6]arene substituted at the upper rim with two or three malondiamide moieties should constitute a promising ligand for lanthanide and actinide cations due to co-operative complexation with the malondiamides. Based on these considerations, we synthesised calix[6]arenes functionalised with malonic acid derivatives.

1. Introduction

The separation of lanthanides and specially actinides from the nuclear fuel and the transmutation of long-lived isotopes to short lived ones are very important for the reprocessing of spent nuclear fuel.

The DIAMEX process in which malondiamides are used as extractants is one of the most promising one because these kind of extractants are well-suited compounds to extract trivalent actinides from nitric acid solutions. On the other hand, they are completely incinerable and have very low water solubility.

Lipophilic malondiamides have been recently employed successfully as extractants for lanthanide and actinide cations from strongly acid media. It has been observed that more than one malondiamide ligands participates in the complexation of each metallic cation [1]. For that reason it was decided to synthesize calix[6]arenes functionalised with malonic acids derivatives.

2. Malondiamide calix[6]arenes

As starting materials for this proposal, a variety of amines on the calixarenes were used with different acyl chlorides.

Amines **1** and **2** were synthesised starting from p-tert-butyl calix[6]arene [2], as described in Figure 1, by successive selective alkylation, nitration, total alkylation of the platform and finally reduction to the desired amine [3].

Figure 1**. Synthesis of amines 1 and 2**

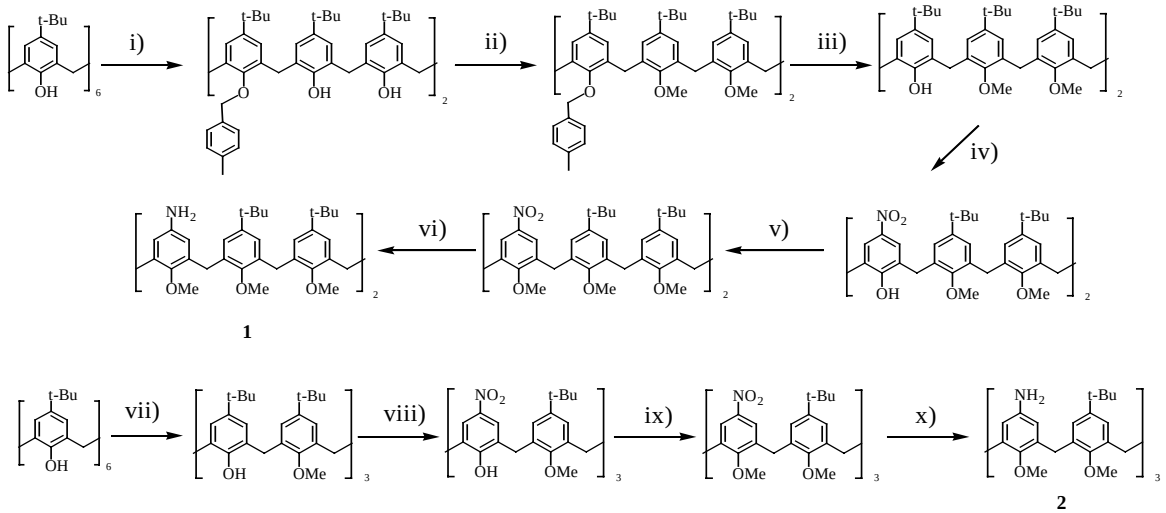

i) Me_3SiOK, $BrCH_2C_6H_4CH_3$.
ii) NaH, Me_2SO_4.
iii) H_2, Pd/C.
iv) HNO_3/H_2SO_4.
v) NaH/Me_2SO_4.
vi) H_2/PtO_2.
vii) Na_2CO_3/IMe.
viii) HNO_3/H_2SO_4.
ix) K_2CO_3/Me_2SO_4, x) H_2/PtO_2.

These compounds were reacted with acyl chlorides **3**, **4** and **5**. Compound **3** is commercially available and compounds **4** and **5** were obtained from commercially available di-esters by monohydrolysis with MeOH/H_2O/KOH followed by treatment of the resulting carboxylic acids with Cl_2SO (Figure 2).

Figure 2. **Formula 3 and synthesis of compounds 4 and 5**

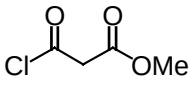

3 Commercially available

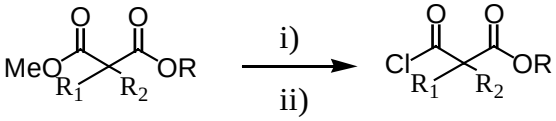

4: R=R_1=Et, R_2=H (88%)
5: R=Me, R_1=R_2=Et (86%)

i) KOH,
ii) Cl_2SO

The reaction of acyl chlorides **3**, **4** and **5** with the amines **1** and **2** in CH_2Cl_2 in the presence of Et_3N at room temperature gave the ester derivatives **6-10** (Figure 3).

Figure 3. **Synthesis of esters 6-10**

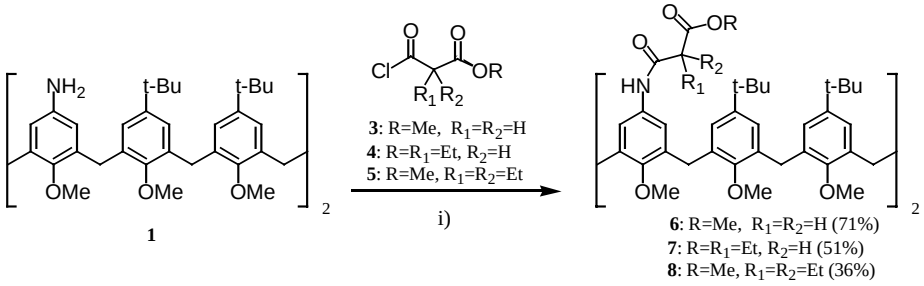

6: R=Me, R_1=R_2=H (71%)
7: R=R_1=Et, R_2=H (51%)
8: R=Me, R_1=R_2=Et (36%)

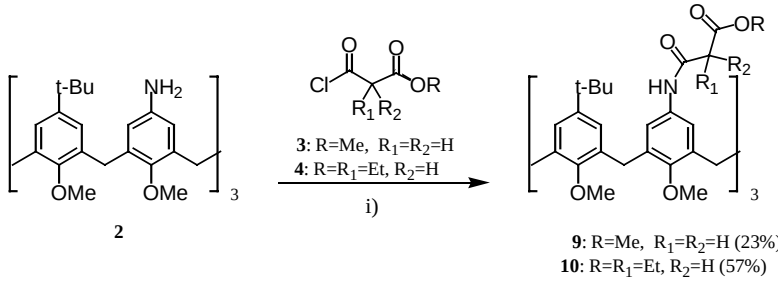

9: R=Me, R_1=R_2=H (23%)
10: R=R_1=Et, R_2=H (57%)

i) Et_3N, CH_2Cl_2, r.t.

Aminolysis of these compounds with butylamine at reflux temperature gave malonamide derivatives **11-15**, as described in Figure 4.

Figure 4. **Synthesis of amides 11-15**

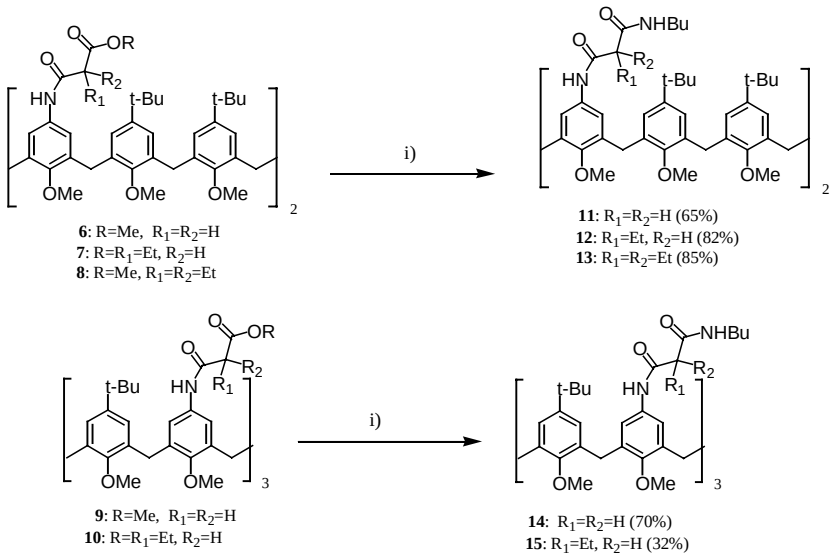

6: R=Me, R_1=R_2=H
7: R=R_1=Et, R_2=H
8: R=Me, R_1=R_2=Et

11: R_1=R_2=H (65%)
12: R_1=Et, R_2=H (82%)
13: R_1=R_2=Et (85%)

9: R=Me, R_1=R_2=H
10: R=R_1=Et, R_2=H

14: R_1=R_2=H (70%)
15: R_1=Et, R_2=H (32%)

i) NH_2Bu/Δ

These compounds are currently being tested in lanthanide-actinide extraction.

Acknowledgements

The work presented in this paper was supported by the Comunidad Autonoma de Madrid and by the European Union (contract F14W6CT 960022).

REFERENCES

[1] a) G.Y.S. Chan, M.C.B. Drew, M.J. Hudson, P.B. Iveson, J.O. Liljenzin, M. Skalberg, L. Spjuth, C. Madic, *Solvent Extraction of Metal Ions From Nitric Acid Solution Using N,N´-substituted Malonamides. Experimental and Crystallographic Evidence for Two Mechanism of Extraction, Metal Complexation and Ion-pair Formation*, J. Chem. Soc., Dalton Trans., 1997, 649-660.

b) P.B. Iveson, M.G.B. Drew, M.J. Hudson, C. Madic, *Structural Studies of Lanthanide Complexes With New Hydrophobic Malonamide Solvent Extraction Agents*, J. Chem. Soc., Dalton Trans., 1999, 3605-3610.

[2] C.D. Gutsche, B. Dhawan, M. Leonis, D. Steward, *p-tert-butyl Calix[6]arene*, Organic Synthesis, 1989, 238.

[3] A. Casnati, L. Domiano, A. Pochini, R. Ungaro, M. Carramolino, J.O. Magrans, P.M. Nieto, J. Lopéz-Prados, P. Prados, J. de Mendoza, R.G. Janssen, W. Verboom, D.N. Reinhoudt, *Synthesis of Calix[6]arenes Partially Functionalised at the Upper Rim*, Tetrahedron, 1995, 51, 12699-12720.

ACTINIDE(III)/LANTHANIDE(III) PARTITIONING USING n-Pr-BTP AS EXTRACTANT: EXTRACTION KINETICS AND EXTRACTION TEST IN A HOLLOW FIBER MODULE

Andreas Geist, Michael Weigl, Udo Müllich, Klaus Gompper
Forschungszentrum Karlsruhe GmbH, Institut für Nukleare Entsorgung
POB 3640, 76021 Karlsruhe, Germany
E-mail: geist@ine.fzk.de

Abstract

2,6-di(5,6-dipropyl-1,2,4-triazin-3-yl)pyridine (n-Pr-BTP), first developed in our laboratory, is a very promising extractant for the effective separation of actinides(III) from lanthanides(III). It is able to extract actinides(III) with usable distribution coefficient from 1-2 molar nitric acid selectively over lanthanides(III). The Am(III)/Eu(III) separation factor is approx. 135. The performance of this extractant is further elucidated by kinetic investigations and a counter-current extraction experiment in a hollow fiber module (HFM). The kinetic investigations were performed in a stirred cell. The fact that extraction rate is independent of stirring speed reveals a slow chemical complexation reaction. The HFM extraction test on americium(III)/fission lanthanides(III) separation showed good hydrodynamic behavior. Depending on aqueous flow rate, which was varied, up to 94% americium could be removed from the feed phase. Lanthanide co-extraction was in the range of 1%.

1. Introduction

Over the recent years, efforts have been made finding extractants capable of separating trivalent actinides from fission lanthanides. This separation task is a key step in the separation of minor actinides from high-level Purex effluents within the P&T strategy [1]. Ideally, such an extractant would selectively extract trivalent actinides over lanthanides from moderately acidic media without the need for pH adjustment or the use of salting-out agents. Furthermore, it would consists only of C, H, O, and N atoms ("CHON principle"), making it fully combustible to gaseous products.

2,6-di(5,6-dipropyl-1,2,4-triazin-3-yl)pyridine (n-Pr-BTP), which was developed in our laboratory [2,3], is an extractant capable of fulfilling this task. It is able to selectively extract actinides(III) over lanthanides(III) from 1-2 molar nitric acid with usable distribution coefficient. Am(III)/Eu(III) separation factor is approx. 135. The extractant complies to the CHON principle.

Figure 1. **2,6-di(5,6-dipropyl-1,2,4-triazin-3-yl)pyridine (n-Pr-BTP)**

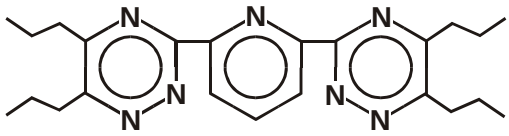

In shaking tubes, equilibrium is not attained very rapidly. We feel that this indicates a slow chemical complexation reaction. To further elucidate the kinetics of extraction, we performed experiments on Am(III) extraction in a stirred cell built specifically for our purposes [4].

A constant-interface, Lewis-type stirred cell is the best tool for extraction kinetics studies, if it is calibrated [5,6]. It allows the discrimination of flow-dependent transport processes (diffusional regime) from flow-independent interfacial reactions (chemical regime) as rate determining alternatives by measuring extraction rates at varied stirring speeds. The cell we used in this work is tested on a physical mass transfer system (toluene transfer into water), showing a linear dependency of mass transfer rate on stirring speed over a wide range [4]. Therefore we can be sure that fluxes independent of stirring speed indicate that an interfacial process (i.e. the chemical reaction) is rate determining.

With n-Pr-BTP, a hot mixer-settler test using a synthetic feed solution and a hot test in a 16-stage centrifugal extractor using genuine DIAMEX raffinate for feed solution were performed in other laboratories [7]. These tests were very successful. Americium(III) and curium(III) could quantitatively be extracted (<99.85%) and almost completely be recovered.

Instead of using the above extraction equipment, we performed an extraction test in a hollow fiber module (HFM). Basically, in a HFM, aqueous and organic phases are macroscopically separated by a micro-porous membrane (usually consisting of hydrophobic membrane material). Phase contact is maintained within the pores by the application of a proper pressure difference (with hydrophobic membrane material, pressure in the aqueous phase is kept slightly higher than in the solvent phase). This yields a wide flexibility towards hydrodynamic conditions, overcoming restrictions often encountered with conventional extractors, e.g. entrainment.

The first application of non-dispersive chemical extraction in a HFM was described some 15 years ago [8]. In the meantime, many publications have followed, however, mainly using well-known extractants. To our knowledge, this is the first HFM extraction test on actinide(III)/lanthanide(III) separation using an "exotic" extractant. Tests like this one should eventually allow one to evaluate the capability of non-dispersive extraction in the field of partitioning.

2. Experimental

2.1 Synthesis and characterisation of n-Pr-BTP

We prepared two batches of 40-50 g n-Pr-BTP each as described in [3]. Melting points were in the range of 105-107°C. NMR data confirmed the products' identities. To further characterise the products, we performed distribution measurements: Contacting a solution of 0.04 M n-Pr-BTP in TPH (a kerosene-type diluent) modified with 1-octanol (70:30 vol.) and 1 M nitric acid labelled with ^{241}Am or ^{152}Eu, we found an americium distribution coefficient of approx. 14 and a separation factor, $SF_{Am(III)/Eu(III)}$ of 135. This is in good agreement with results published elsewhere [7].

2.2 Extraction kinetics

Kinetic measurements were performed in our special small stirred cell. Its half cell volume is only 60 mL [4]. The aqueous phase was a solution of americium(III) (2 500 Bq/mL) in 1 M nitric acid. Organic phase was a solution of 0.04 M n-Pr-BTP in TPH/1-octanol (70:30 vol.).

The stirred cell was filled with both aqueous and organic phases, and stirrers were started with appropriate stirring speeds (aqueous = organic). The activity in the aqueous phase was continuously detected in a by-pass with a well-type NaI-detector. Measured activity was plotted vs. time and initial metal fluxes were calculated.

2.3 HFM extraction test

2.3.1 Feed solutions

Aqueous feed contained ^{241}Am(III), fission lanthanides(III) and yttrium(III). Its composition corresponds to a DIAMEX raffinate as used in other n-Pr-BTP tests [7], except that ^{241}Am was used in trace amount, and Cm, Ru, Pd, Fe were not present. The composition is given in Table 1. The organic phase was a solution of n-Pr-BTP (0.04 kmol/m^3, 16.2 g/L) in TPH/1-octanol (70:30 vol.).

Table 1. **Composition of aqueous feed solution**

HNO_3	1.0 kmol/m^3
Y	89.0 mg/L
La	294 mg/L
Ce	566 mg/L
Pr	264 mg/L
Nd	998 mg/L
Sm	199 mg/L
Eu	35.7 mg/L
Gd	28.2 mg/L
^{241}Am	0.49 MBq/L

2.3.2 Set-up

We set up a single HFM extractor inside a glove box. This corresponds to the extraction stages in commonly used extractor batteries, without scrubbing or stripping stages. The HFM set-up is shown schematically in Figure 2. Both phases were passed through the module in counter-current, single-pass mode, i.e. phases were not recycled. The organic phase flowed in the lumen of the hollow fibers (HF). The module used was a Celgard LiquiCel Extra-Flow type module (10 000 HF, membrane material polypropylene, average pore size 0.02 µm, porosity ε = 40%, tortuosity τ = 2.6 [9], HF inner diameter = 0.24 mm, HF outer diameter = 0.30 mm, active length = 0.15 m). Static pressure in the aqueous phase was kept approx. 0.5 bar higher than in the organic phase to maintain proper phase separation. Aqueous flow rate was varied, 0.44 L/h•Q_{aq}•1.75 L/h, organic flow rate was kept constant at Q_{org} = 0.50 L/h. Further details can be found in [10].

Figure 2. **Single-pass, counter-current HFM set-up (schematic). —— aqueous phase, - - - organic phase, PI = pressure gauge, FI = flow meter (rotameter), CV = control valve, BP = bypass valve**

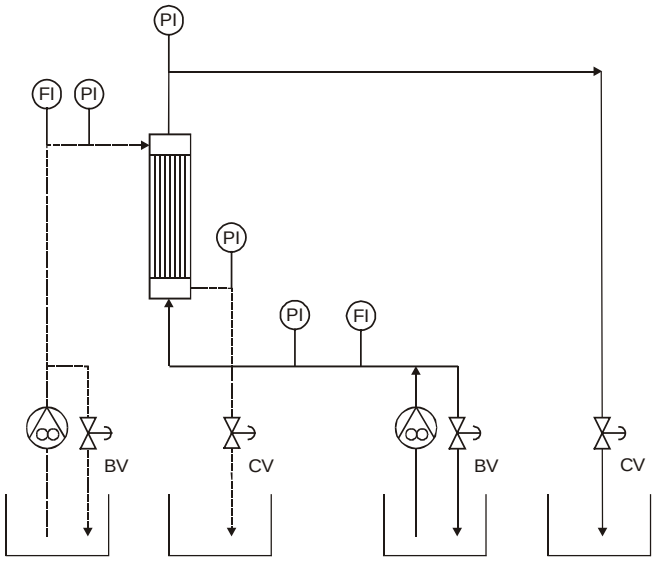

2.3.3 Analytic

Samples of aqueous and organic effluents were drawn discontinuously. ^{241}Am γ activitiy was determined on a γ counter (*Packard Cobra Auto-Gamma*). Lanthanide concentrations were measured with ICP-AES after proper dilution with nitric acid (aqueous samples) or stripping into 0.01 nitric acid (organic samples).

3. Results

3.2. Extraction kinetics

The plot of normalised initial americium fluxes, $j_{t=0}$ /$[Am^{3+}]_{t=0}$, (Figure 3) characterises the kinetic behaviour of americium extraction with n-Pr-BTP. The flow-independent fluxes (plateau rates) indicate that the interfacial reaction is rate determining (i.e. non-equilibrium at the interface).

Figure 3. **Americium(III) extraction into n-Pr-BTP. Stirring rate dependency of normalised initial americium fluxes.**
[Am^{3+}] = 2500 Bq/mL, [HNO_3] = 1.0 kmol/m^3, [*n-Pr-BTP*] = 0.04 kmol/m^3.

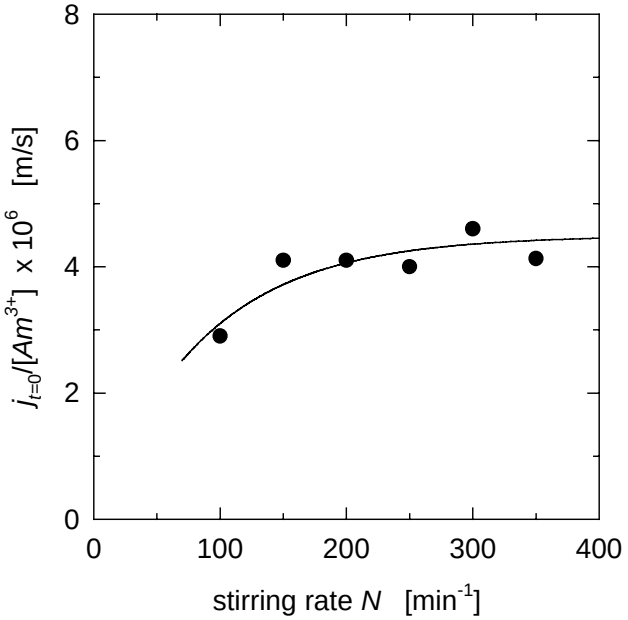

This means that mass transfer is chemically controlled. This case is very interesting as it allows studying the mechanism of the interfacial reaction. Therefore the dependency of the plateau rate from the concentrations of all participating species (Am^{3+}, H^+, NO_3^-, n-Pr-BTP) must be studied. This leads to the reaction orders of the interfacial reaction for each species. If the reaction orders are known a rate equation can be expressed.

Some preliminary measurements indicate a first order dependency on the concentration of n-Pr-BTP. The measurements for the other species are still in progress, therefore a mechanism for the americium extraction with n-Pr-BTP cannot be postulated yet.

3.2. HFM extraction test

Throughout the experiment, which ran four hours, the hydraulic behaviour was highly satisfactory, i.e. both aqueous and organic effluents were clear without any entrainment. This is a benefit of the macroscopic phase separation by the membrane material.

Except with an aqueous flow rate of Q_{aq} = 0.44 L/h, mass balances were (100 ± 2.5)% for lanthanides, and 90-98% for Am(III). With an aqueous flow rate of 0.44 L/h, Am(III) mass balance was 66%, lanthanides mass balances were approx. 88%. This is a sign that, at this flow rate, the experiment was not run sufficiently long to reach steady state.

Aqueous effluent concentrations normalised to feed concentrations, $[Me^{3+}]_{out}/[Me^{3+}]_{in}$, over aqueous flow rate, Q_{aq}, are shown in Figure 4. With an aqueous flow rate of 0.44 L/h, 94% of Am(III) could be removed from the aqueous phase. There is a strong dependency of Am(III) extraction efficiency on aqueous flow rate, and hence residence time: With an aqueous flow rate of 1.75 L/h, only 40% of Am(III) could be extracted. The steep flow rate dependency indicates that, at significantly

lower flow rates, Am(III) would be extracted almost quantitatively. However, the experimental set-up, regarding the pumps, control valves and flow indicators installed, was not layed out for such low flow rates.

Figure 4. **Am(III)/Ln(III) separation in a HFM using n-Pr-BTP as extractant. Relative aqueous effluent concentrations as a function of aqueous flow rate. Aqueous phase, shell-side: Am(III) + Ln(III) in HNO_3 1.0 kmol/m^3. Organic phase, in HF: [*n-Pr-BTP*] = 0.04 kmol/m^3 in TPH/1-octanol (70:30 vol.). Q_{org} = 0.50 L/h.**

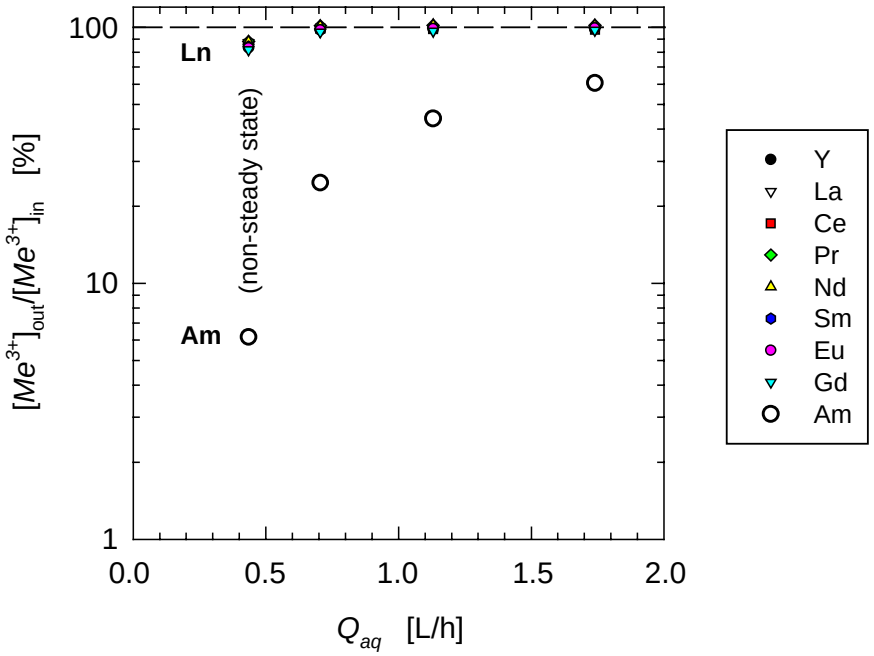

Except for the non-steady state result with an aqueous flow rate of 0.44 L/h, no lanthanide co-extraction was detectable in the aqueous phase. Lanthanide co-extraction as determined from organic effluent samples was in the range of 1-2% for Sm, Eu, Gd, and well below 0.5% for other lanthanides. We point out these good results concerning lanthanide co-extraction were realised without lanthanide scrubbing, due to the high separation factor of n-Pr-BTP.

4. Conclusion

n-Pr-BTP is a very capable extractant for An(III)/Ln(III) separation from acidic media. Although Am(III) extraction rate is not very fast, results from a HFM extraction experiment are promising. Operation is stable, lanthanide co-extraction is small. Still better results can be expected from a modified experimental set-up which can handle lower flow rates. Tests on lanthanide scrubbing and back extraction will be performed to further evaluate the behaviour of the n-Pr-BTP extraction system in a hollow fiber module.

Acknowledgements

The authors would like to thank the European Commission for their financial support.

REFERENCES

[1] OECD Nuclear Energy Agency, *Status and Assessment Report on Actinide and Fission Product Partitioning and Transmutation,* (1999), (www.nea.fr/html/pt/pubdocs.htm).

[2] Z. Kolarik, U. Müllich and F. Gassner, *Selective Extraction of Am(III) Over Eu(III) by 2,6-Ditriazolyl- and 2,6-Ditriazinylpyridines,* Solvent Extr. Ion Exch. 17, 23 (1999).

[3] Z. Kolarik, U. Müllich and F. Gassner, *Extraction of Am(III) and Eu(III) Nitrates by 2,6-Di(5,6-dipropyl-1,2,4-triazin-3-yl)pyridine,* Solvent Extr. Ion Exch. 17, 1155 (1999).

[4] M. Weigl, A. Geist, K. Gompper, J.I. Kim, *Kinetics of Lanthanide/Actinide Co-extraction with N,N'-dimethyl-N,N'-dibutyltetradecylmalonic diamide (DMDBTDMA)* (submitted).

[5] G.J. Hanna, R.D. Noble, *Measurement of Liquid-liquid Interfacial Kinetics,* Chem. Rev. 85, 583 (1985).

[6] P.R. Danesi, Chapter 5 in: *Principles and Practices of Solvent Extraction,* J. Rydberg, C. Musikas, G.R. Choppin (Eds), Marcel Dekker Inc., New York, Basel, Hong Kong (1992).

[7] C. Madic *et al.*, *New Partitioning Techniques for Minor Actinides,* Final Report, EUR-19149 (2000).

[8] B.M. Kim, *Membrane-based Solvent Extraction for Selective Removal and Recovery of Metals,* J. Membr. Sci. 21 (1984) 5.

[9] R. Prasad, K.K. Sirkar, *Dispersion-free Solvent Extraction With Microporous Hollow-fiber Modules,* AIChE J. 34 (1988) 177.

[10] U. Daiminger, A. Geist, W. Nitsch, P. Plucinski, *The Efficiency of Hollow Fiber Modules for Non-dispersive Chemical Extraction,* Ind. Eng. Chem. Res. 35, 184 (1996).

THE POTENTIAL OF NANO- AND MICROPARTICLES FOR THE SELECTIVE COMPLEXATION AND SEPARATION OF METAL IONS/RADIONUCLIDES

C. Grüttner[1], S. Rudershausen[1], J. Teller[1], W. Mickler[2], H.-J. Holdt[2]
[1]Micromod Partikeltechnologie GmbH, Friedrich-Barnewitz-Str. 4,
18119 Rostock, Germany,
E-mail: www.micromod.de

[2]Universität Potsdam, Institut für Anorganische Chemie,
Am Neuen Palais 10, Haus 9, 14469 Potsdam, Germany

Abstract

Nano- and microparticles for the selective complexation of metal ions and especially radionuclides on their surface are presented. Beside several applications of such magnetic and non-magnetic particles in the fields of biomedicine, diagnostics, molecular biology, bioinorganic chemistry and catalysis a high potential exists for the complexation of radionuclides from nuclear wastewater on particle surfaces. The magnetic properties of nano- and microparticles allow the fast magnetic separation of radionuclides from the radioactive liquid waste stream, for example. The removal of radionuclides from strongly acidic wastes requires a high stability of the particles in combination with the protection of the incorporated iron oxide. The covalent binding of selective chelators allows the fractionation of different types of radionuclides regarding the special needs of nuclear waste treatment.

1. Introduction

Nano- and microparticles are widely used for the immobilisation of metal ions [1] and radionuclides [2,3] in the fields of biomedicine [4], molecular biology [5], medical diagnostics [6], bioinorganic chemistry and catalysis [7]. In general there are two possibilities for the binding of metal ions on particle surfaces. One method is based on the simple physical adsorption of chelators [8] or metal ions on particle surfaces by inclusion into pores of the particles, adhesion processes or electrostatic interactions The second more specific method consists of the complexation of metal ions by selective chelators which are covalently attached to the particle surface. Nearly all applications of the metal ion immobilisation on particle surfaces require an efficient complexation of the metal ions to prevent traces of free metal ions in the special medium. Therefore the effective chemical binding of metal ions on particle surfaces is our method of choice.

Here we report our results on the selective binding of metal ions and radionuclides on the surface of magnetic and non-magnetic particles for the application in the magnetic field assisted radionuclide therapy, for the selective binding of histidine-tagged proteins via the formation of a nickel(II) protein complex, and for the complexation of palladium ions by sulfur-rich macrocyclic ligands on the surface of silica particles.

These experiences resulting from the immobilisation of metal ions and especially radionuclides for life sciences applications initiated our first attempts of the selective complexation of lanthanides and actinides on the surface of magnetic silica beads. Current approaches for the recovery of lanthanides and actinides from high level nuclear waste are based on the TRUEX process which utilises the highly efficient, neutral, organophosphorous ligand octyl-phenyl-*N*,*N*-diisobutyl-carbamoylmethyl-phosphine oxide (CMPO) [9]. Previously, calix[4]arene based extractants which incorporate CMPO moieties at either the wide [10,11] or narrow rim have been reported [12]. Such pre-organisation of the chelating ligands leads to a 100 fold (or even more) increase [10] in extraction efficiency combined with an enhanced selectivity for actinides and lighter lanthanides [13]. Derivatives with single CMPO groups and CMPO-substituted calixarenes were covalently attached to the surface of magnetic silica particles allowing controlled ligand loading with defined orientation [14].

First solid-liquid extraction experiments were performed under conditions that simulate European nuclear waste streams (4M $NaNO_3$, 1M HNO_3). Separation of europium, cerium or americium, as representatives of the early lanthanides and actinides, was evaluated. ICP-MS measurements of the initial nuclide activity in the aqueous phase and the activity after shaking with the particles were used to calculate the percentage extraction [14].

2. Selective complexation of the radionuclides ^{99m}Tc/^{188}Re and ^{111}In/^{90}Y on the surface of microparticles for therapeutical purposes

The magnetic field assisted radionuclide therapy aims the targeting of diagnostically and therapeutically important radionuclides like ^{99m}Tc or ^{111}In and ^{188}Re or ^{190}Y, respectively, to the tumour. Therefore the radionuclides are efficiently complexed on the surface of biocompatible magnetic nanoparticles. These nanoparticles are injected in the near of the tumor region and kept in the target area by means of external magnetic fields. This leads to a high concentration of radioactivity at the tumor and prevents side effects on the healthy tissue [15]. Another strategy for successful tumour treatment is the intracavitary radionuclide therapy: The radioactive labelled microspheres are immobilised in the tumour because of their size, and irradiate the tumour cells. After the radioactivity is faded away the microspheres are biotransformed into harmless metabolites [16]. Both strategies ideally require magnetic or non-magnetic biodegradable particles able to complex radionuclides

efficiently and stable. This can be reached by reacting one of the best known chelators for technetium and rhenium, MAG_3 **1**, or for indium and yttrium, DOTA **2**, with a functionality, e.g. an amino group, on the surface of the microsphere (Schemes 1 and 2).

Scheme 1. **Chemical structures of mercaptoacetyl-triglycine (MAG_3) [17] 1 and 1,4,7,10-tetraazacyclododecane-N,N',N'',N'''-tetraacetic acid (DOTA) [18] 2**

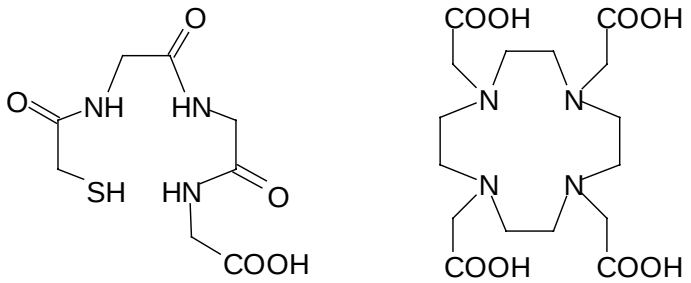

1 **2**

Scheme 2. **Covalent binding of chelators to particle surfaces followed by radiolabeling**

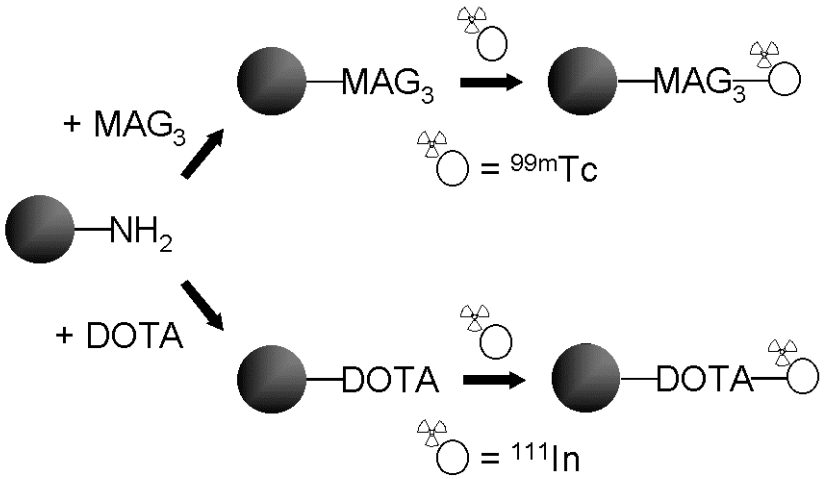

Then these microspheres can either be labelled with the radioactive isotopes ^{99m}Tc or ^{111}In, which are gamma emitters, or with the beta emitters ^{188}Re or ^{90}Y for therapeutic applications. In the case of ^{99m}Tc we obtained first results for non-magnetic microspheres with a labeling efficiency (particle-bound activity) of 39% and an *in-vitro* stability of the particle bound MAG_3-technetium complex of 79%. A relatively high labelling efficiency of non-magnetic microspheres of 72% and an *in-vitro* stability of more than 90% could be reached with the gamma emitter ^{111}In.

In future we want to optimise the labelling procedure, develop new chelators for technetium, rhenium, indium and yttrium and investigate a combination of the intracavitary radionuclide therapy with the strategy of the magnetic drug targeting.

3. Selective removal of histidine-tagged proteins from fermentation solutions by nickel(II)-protein complex formation on the surface of magnetic silica particles (sicastar®-M)

The covalent binding of backbone-modified nitrilotriacetic acid (NTA) on the surface of magnetic silica particles is the basis for the formation of a nickel(II) complex with a high complex stability. The backbone-modification allows the interaction of four chelating sites of the modified NTA with nickel(II) ions, which results in a more tightly binding of nickel(II) ions in comparison to systems with only three sites available for the nickel(II) complexation (Scheme 3).

Scheme 3. **a) Interaction of four donor atoms of backbone modified NTA with nickel(II) ions, b) Interaction of only three donor atoms of non-modified NTA with nickel(II) ions. One carboxylic acid group of the NTA is necessary for the covalent binding on the particle surface.**

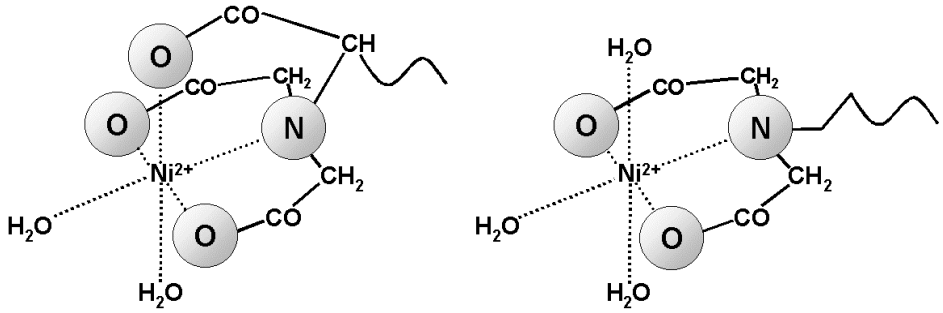

The high selectivity of this Ni(II)-NTA complex for proteins with an affinity tag of six consecutive histidine residues allows a one-step purification of almost any protein from any expression system under native or denaturing conditions (Scheme 4).

Scheme 4. **Principle of the selective binding of his-tagged proteins on the surface of particles containing chelated metal ions (nickel(II) ions) on the surface.**

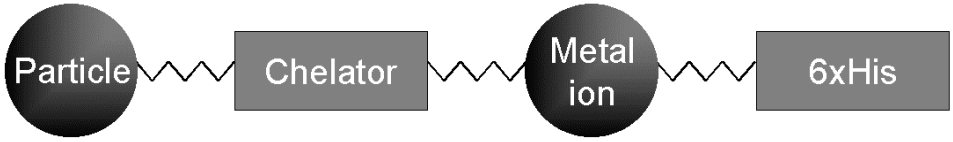

Electrokinetic measurements of the surface potential of magnetic silica beads have been carried out to determine the optimal density of NTA on the surface of the particles. Therefore the density of NTA was increased stepwise until a saturation of the surface with NTA was achieved. This saturation range was detected by the comparison of the Zetapotential values of the particles at a constant pH-value of 8.0 (Figure 1a). In addition streaming potential measurements were carried out to determine the corresponding particle charge density values by polyelectrolyte titration against 0.001 N poly(diallyldimethylammonium chloride) (Figure 1b). An optimal surface was realised by reacting 250-500 µmol NTA-chelator with one g of functionalized particles. The binding capacity of the optimized NTA-modified particles lies in the range of 2.5-3.0 nmol nickel(II) ions per g of magnetic silica particles. The magnetic silica-NTA beads (sicastar® -M) can be used to purify 6xHis-tagged proteins from any expression system including baculovirus, mammalian cells, yeast, and bacteria.

Figure 1a. **Zetapotential of NTA-modified silica particles (sicastar®-M) with increasing densities of NTA-groups on the surface (electrolyte: 10^{-4} M KCl, pH = 8.0)**

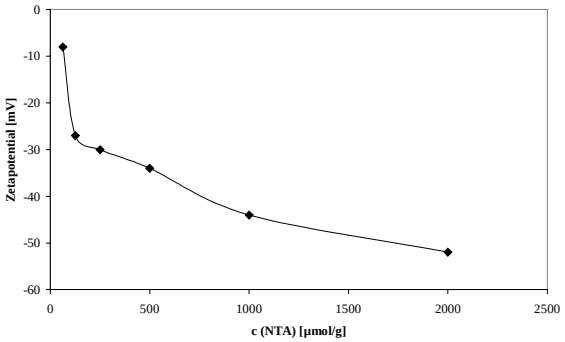

Figure 1b. **Particle charge density of NTA-modified silica particles (sicastar®-M) with increasing densities of NTA-groups on the surface measured by polyelectrolyte titration against 0.001 N poly(diallyldimethylammonium chloride).**

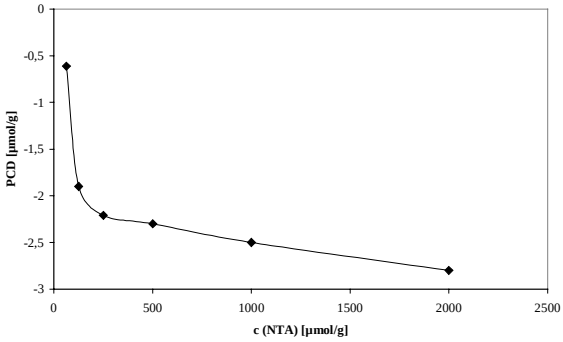

4. Complexation of palladium ions by sulfur-rich macrocycles on the surface of silica particles

1,2-Dithioethenes are weak chelate-forming ligands [19]. In the case of bis(methylthio)maleonitrile [20] the donor power of the sulphur atoms is further decreased by the electron withdrawing effect of the cyano groups. Crowned dithiomaleonitriles are macrocyclic chelate ligands which extract Pd(II) at sufficient rate in a very good yield. The reason for that extraction behaviour is the fact that Pd(II) favours the square planar coordination geometry in opposite to the 3d-metals and thiophilic d^{10} ions like Ag(I) and Hg(II).

For the synthesis of the immobilised ligands the 2-allyloxy-1,2-propanediol is transformed into the dichloro compound, which is reacted with a dithiolate ((Z)1,2-disodium-1,2-dicyanethene-1,2-dithiolate, 1,2-disodium-4-methylbenzene-1,2-dithiolate [21]) at high dilution conditions yielding the macrocycle. Than the allylsubstituted crown ether is silylated and the resulting alkoxysilane is immobilized on activated silica beads (Scheme 5).

Scheme 5. **Derivatization of the macrocycle for the immobilization on silica beads**

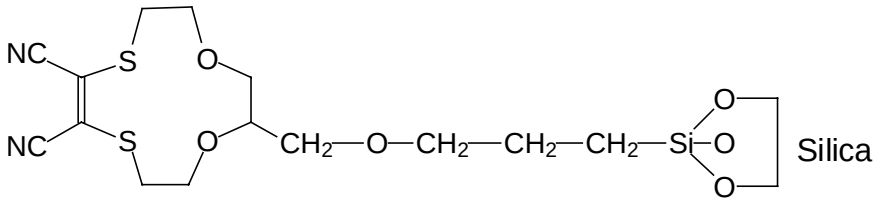

The substituent forms simultaneously a spacer which can be modified in the future. The selectivity of the ligand should be applied by immobilisation at an inactive matrix for the accumulation of Pd(II) from diluted solutions. The extraction of Pd(II) was performed from nitric acid solution with a yield of 93% into a ligand solution (chloroform, kerosene). The extraction equilibrium is reached after 10 min. By AAS the metal concentration in the aqueous phase was determined to calculate the extraction rate.

Scheme 6. **Formation of the macrocycle-Pd(II) complex**

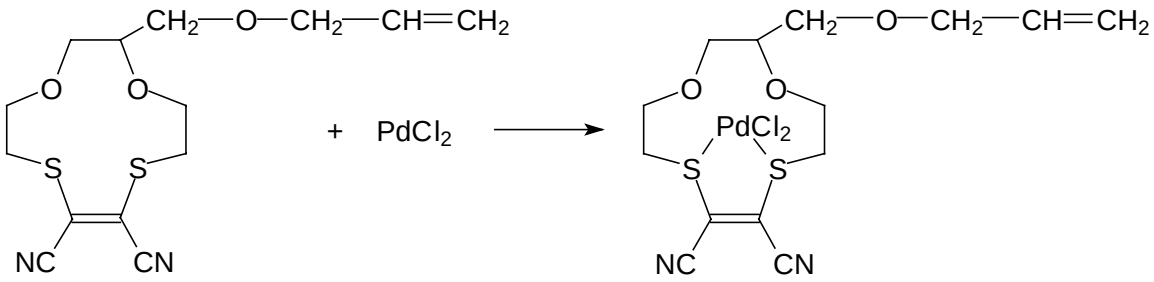

The extraction rate increases from the acyclic compound through maleonitrile-dithio-21-crown-7, maleonitrile-dithio-15-crown-5 and maleonitrile-dithio-18-crown-6 by modification of the cavity of the macrocycle. The best results can be observed for the maleonitrile-dithio-12-crown-4. The rise of the function lg D = f(lgc_L) gives the composition of the extracted compounds as 1:1. Summarising, a very good separation of Pd(II) can be specified from 3d-metals and other thiophilic metal ions. In addition to the extraction experiments and the crystal structures the formation constants of selected chelates were determined by UV spectroscopy. The observed order corresponds to that found by the extraction of palladium in the system water/chloroform.

5. Extraction of lanthanides and actinides by magnetically assisted chemical separation technique

The removal of radionuclides from strongly acidic wastes requires a high stability of the particles in combination with the protection of the incorporated iron oxide. Therefore magnetic silica particles were additionally coated with functionalized alkoxysilanes to encapsulate the iron oxide and to introduce functional groups for the covalent binding of chelators on the particle surface.

Carboxylic acid modified sicastar®-M (**I**) were used as the basis for the attachment of simple CMPO ligands directly onto the particle surface (**II**). The CMPO-modified particles (**II**) enable extraction of ^{152}Eu, ^{241}Am and ^{139}Ce albeit at a very low level only slightly higher than with **I** (Scheme 7, Table 1). However, the calix[4]arene based particles (**III**), with a roughly identical concentration of ligating functions, show a significantly higher level of extraction (Scheme 7, Table 1). This demonstrates the importance of pre-organization of the chelating ligands on a suitable macrocyclic scaffold, prior to their attachment at the particle surface [14].

Table 1. **Percentage extraction after 19 h shaking**

Magnetic silica particles	**^{152}Eu**	**^{241}Am**	**^{139}Ce**
I	3.7%	<1%	9%
II	1.5%	0.4%	7.5%
III	77.6%	81.7%	91.6%

Scheme 7. **Magnetic silica particles (sicastar®-M) with carboxylic acid groups (I), CMPO-derivatives (II), and calix[4]arenes with pre-organised CMPO-derivative units (III) on the particle surface**

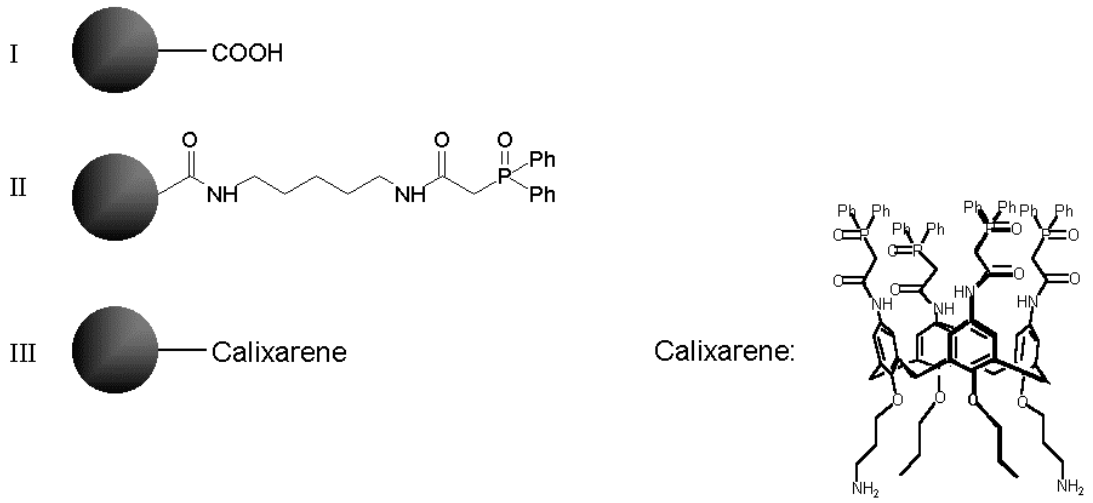

Partition coefficients comparable to those seen for the systems with adsorbed ligands [8] are obtained for europium extraction. However, in contrast, larger K_D values per mass of ligating function are found for americium. Thus the covalent systems show considerably enhanced extraction of americium over europium and offer the potential of selective separation. This reinforces the importance of initial pre-organisation in imparting selectivity. CMPO extractants, such as octyl phenyl *N*,*N*-diisobutyl carbamoylmethyl phosphine oxide are unable to discriminate greatly between actinides and lanthanides showing only a slight preference for the heavier lanthanides. In contrast, it has previously been shown, with non-particulate systems [10,11], that incorporation onto a calix[4]arene allows differentiation between the actinides and lanthanides based on their cationic radii; the actinides and lighter lanthanides with larger radii being extracted more efficiently. The ease of separation of magnetic particles from the waste stream using magnetic fluidised bed techniques makes this system more attractive for future industrial development.

6. Conclusion

Nano- and microparticles have a high potential for the selective binding of metal ions on their surface. Thus the particles can be applied in different fields by variation of the particle matrix, the particle size and chelators, which are covalently bound on the particle surface. Beside the established particle use in the life sciences and chemistry the special application of magnetic nano- and microparticles increases for the removal of heavy metal ions and radionuclides from wastewater.

REFERENCES

[1] M.D. Kaminski, and L. Nunez, *Extractant-coated Magnetic Particles for Cobalt and Nickel Recovery from Acidic Solution*, J. Magn. Magn. Mat., 1999, 194, 31-36.

[2] L. Nunez, B.A. Buchholz, and G.F. Vandegrift, *Waste Remediation Using in-situ Magnetically Assisted Chemical Separation*, Separation Sci. Technol., 1995, 30, 1455-1471.

[3] S.A. Slater, D.B. Chamberlain, S.A. Aase, B.D. Babcock, C. Conner, J. Sedlet, and G.F. Vandegrift, *Optimization of Magnetite Carrier Precipitation Process for Plutonium Waste Reduction*, Separation Sci. Technol., 1997, 32, 127-147.

[4] U.O. Häfeli, S.M. Sweeney, B.A. Beresford, J.L. Humm, and R.M. Macklis, *Effective Targeting of Magnetic Radioactive ^{90}Y-microspheres to Tumour Cells by an Externally Applied Magnetic Field. Preliminary in vitro and in vivo Results*, Nucl. Med. Biol. Int. J. Rad. Appl. Instr. Part B, 1995, 22, 147-155.

[5] J. Gu, C.G. Stephenson, and M.J. Iadarola, *Recombinant Proteins Attached to a Nickel-NTA Column: Use in Affinity Purification of Antibodies*, Bio Techniques, 1994, 17, 257.

[6] W.P. Sisk *et al.*, *High-level Expression and Purification of Secreted Forms of Herpes Simple Virus Type 1 Glycoprotein gD Synthesized by Baculovirus-infected Insect Cells*, 1994, 68, 766.

[7] D.S. Shephard, W. Zhou, T. Maschmeyer, J.M. Matters, C.L. Roper, S. Parsons, B.F.G. Johnson, and M.J. Duer, *Ortsspezifische Derivatisierung von MCM-41: Molekulare Erkennung und Lokalisierung funktioneller Gruppen in Mesoporösen Materialien durch hochauflösende Transmissionselektronenmikroskopie*, Angew. Chem., 1998, 110, 2847-2851.

[8] M. Kaminski, S. Landsberger, L. Nuñez, and G. F. Vandegrift, *Sorption Capacity of Ferromagnetic Microparticles Coated with CMPO*, Separation Sci. Technol., 1997, 32, 115-126.

[9] E.P. Horwitz, D.G. Kalina, H. Diamond, D.G. Vandegrift, and W.W. Schultz, Solv. Extr. Ion Exch., 1985, 3, 75.

[10] F. Arnaud-Neu, V. Böhmer, J.F Dozol, C. Grüttner, R.A. Jakobi, D. Kraft, O. Mauprivez, H. Rouquette, M.J. Schwing-Weill, N. Simon, and W. Vogt, J. Chem. Soc., Perkin Trans. 2, 1996, 1175.

[11] S.E. Matthews, M. Saadioui, V. Böhmer, S. Barboso, F. Arnaud-Neu, M.J. Schwing-Weill, A. Garcia-Carrera, J.F. Dozol, J. Prakt. Chem, 1999, 341, 264.

[12] S. Barboso, A. Garcia-Carrera, S.E. Matthews, F. Arnaud-Neu, V. Böhmer, J.F. Dozol, H. Rouquette, M.J. Schwing-Weill., J. Chem. Soc., Perkin Trans. 2, 1999, 719.

[13] L.H. Delmau, N. Simon, M.J. Schwing-Weill, F. Arnaud-Neu, J.F. Dozol, S. Eymard, B. Tournois, V. Böhmer, C. Grüttner, C. Musigmann, and A. Tunayar, Chem. Commun., 1998, 1627.

[14] S.E. Matthews, P. Parzuchowski, A. Garcia-Carrera, C. Grüttner, J.F. Dozol, and V. Böhmer, *Extraction of Lanthanides and Actinides by Magnetically Assisted Chemical Separation Technique*, Chem. Commun., 2000, submitted.

[15] C. Grüttner, J. Teller, W. Schütt, F. Westphal, C. Schümichen, and B.-R. Paulke, *Preparation and Characterisation of Magnetic Nanospheres for in vivo Application*, in: Scientific and clinical applications of magnetic carriers (Eds. U. Häfeli *et al.*), 1997, Plenum Press, 53-67.

[16] U.O. Häfeli, S.M. Sweeney, B.S. Beresford, E.H. Sim, R.M. Macklis, *Biodegradable Magnetically Directed ^{90}Y-microspheres: Novel Agents for Targeted Intracavitary Radiotherapy*, J. Biomed. Mat. Res., 1994, 28, 901-908.

[17] D.L. Nosco, R.G. Manning, and A. Fritzberg, *Characterisation of the New ^{99m}Tc Dynamic Renal Imaging Agent: MAG_3*, J. Nucl. Med., 1986, 27, 939.

[18] O.A. Gansow, *Newer Approach to the Radiolabelling of Monoclonal Antibodies by Use of Metal Chelates*, Nucl. Med. Biol. Int. J. Rad. Appl. Instr. Part B, 1991, 18, 369-381.

[19] G.N. Schrauzer, H.N. Rabinowitz, J. Am. Chem. Soc., 1968, 90, 4297.

[20] G. Bähr, G. Schleitzer; Chem. Ber., 1957, 90, 438.

[21] H.-J. Holdt, Pur. Appl. Chem., 1993, 445.

NEW EXTRACTANTS FOR PARTITIONING OF FISSION PRODUCTS

J. Plešek, B. Grüner, J. Báča
Institute of Inorganic Chemistry, Rež, Czech Republic

P. Selucký, J. Rais, N.V. Šistková
Nuclear Research Institute Rež, Rež, Czech Republic

B. Časenský
Katchem, Rež, Czech Republic

Abstract

New progress made in the field of dicarbollide [*closo-commo*-(1,2-$C_2B_9H_{11}$)$_2$-3Co)]$^-$ (COSANs) based extractants for partitioning of fission product from spent nuclear fuel, especially Sr^{2+} and actinides, made during past years in the Czech Republic, are described in the paper. The synthetic methods for two classes of new extraction agents containing in the molecule either hydrophobic arylene bridge substituents or metal selective groups with donor atoms able to co-ordinate polyvalent cations have been developed. The structures of the recently prepared extraction reagents are presented, along with ideas on which syntheses were based and the basic relations between structures and extraction properties of the compounds.

1. Introduction

Extraction process for removal of ^{137}Cs and ^{90}Sr from radioactive waste, based on cobaltadicarbollide anion [*closo-commo*-(1,2-$C_2B_9H_{11}$)$_2$-3Co)]$^-$ (COSANs) (see Figure 1) derivatives as extractants, was designed by IIC ASCR and NURI Re in 1972 and further developed during subsequent decade [1-4]. The parent COSAN was later chlorinated in order to protect positions B(8) and B(8') of the cage toward oxidation. The hexachloroderivative, [(8,9,12-Cl_3-$C_2B_9H_8$)$_2$-3-Co]$^{(-)}$-COSAN was found appreciably more stable towards HNO_3, radiation, and even more hydrophobic than the parent compound. Drawback of chlorinated COSANs based process lies, however in the use of polar and environmentally dangerous solvents i.e. nitrobenzene, or halogenated hydrocarbons. Presently, there is a co-operative research on this technology between USA and Russia, but details in the open literature are scarce [5]. In Russia, a plant based on a modified process based on Russian-Czech Patent [6] was launched in autumn 1996.

Figure 1. **Schematic structure of the parent [*closo-commo*-(1,2-$C_2B_9H_{11}$)$_2$-3Co)]$^-$ (COSAN) anion (for clarity, terminal hydrogen atoms are omitted)**

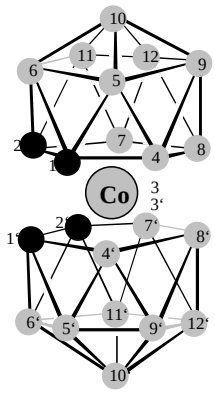

The targets of the recent and current investigations proceeding under framework of two INCO-Copernicus EEC Projects [7] have been directed to find more powerful extractants effective also for actinides and to minimise environmental risks, i.e. they should be able to meet with the EEC ecological requirements. New extractants of closo-borate type have been tailored with the aim to find selective reagents for individual fission products and to improve solubility of boron type extractants in solvents ecologically more acceptable than nitrobenzene, originally used in the above-mentioned dicarbollide process. Two groups of extractants were prepared starting both from sandwich skeleton of COSAN incorporating hydrophobic and selective substituents into extractant molecule.

2. Results and discussion

During past years, attention has been paid on the increase of the hydrophobicity of the molecules introducing arylene rings (phenyl (**1**), tolyl (**2**), ethylbenzyl (**3**), xylyl (**4**), biphenyl (**5**), tetraline (**6**), etc.) bonded in positions 8,8' of the COSAN molecule as a bridge substituents (see Figure 2, for example). Extraction experiments proved that several promising extractants were successfully prepared. The novel class of 4,8', 8,4'- R_2-Bis-arylene bridged COSANs (R = Ph (**7**), R = tolyl (**8**), R = ethylphenyl (**9**)), and especially the basic member of the series bisphenylene-COSAN (**7**), exhibit extreme complexation properties for caesium cation, overcoming significantly extraction ability of dicarbollide itself and displaying enhanced solubility in aromatic solvents. Indeed, bis-bridged class

of COSAN derivatives allowed for use of aromatic solvents (toluene, xylene, etc.) in extraction, provided that some aromatic sulfo compounds were added to the organic phase as so-called "solubilizers" [7]. X-ray studies of the Cs^+ complex of the anion (**7**) revealed, that that the angle 72^o between planes of phenylene substituents of this species is very favourable in order Cs^+ cation can be strongly captured [8]. Distribution ratio of Cs^+ using above anions has been found so high, that imposes a consecutive problem of its back-extraction. This could be only accomplished using nitric acid of high concentration. On the other hand, in comparison with chlorinated COSANs, these compounds seem less stable towards oxidation effect of nitric acid. According to the preliminary extraction studies it seems that addition of urea to the extraction system would probably suppress this effect.

Figure 2. **Schematic structures of the 8,8' phenylene – COSAN (1) and 4,8', 8,4' – bis-phenylene bridged COSAN (7)**

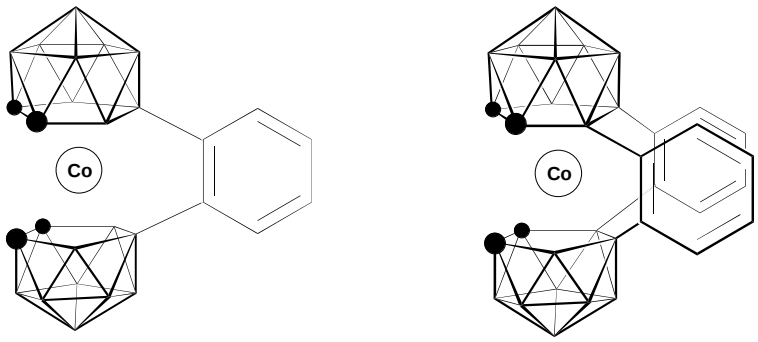

The present study is devoted to COSAN and hydroborate based extractants containing selective groups, including phenoxy groups, linear polyethyleneglycol chains, crown ethers and phosphorus containing moieties, which should allow for selective transfer of strontium and especially M^{3+} and M^{4+} lanthanides and actinides into low polar organic phase without use of any additive.

The target syntheses are based on the idea originated from our previous experience in the synthesis and testing of a large number of borate extractants. According to our knowledge, the polyvalent cations M^{3+} and M^{4+} can be effectively extracted only provided that the anionic COSAN-based extractant amalgamates in one molecule both, hydrophobic anionic part, and a ligating selective moiety containing electron donor atoms, i.e. oxygen, phosphorus, sulphur, etc. able of tight co-ordination to the cation. Such functionalised anionic particles are able to build up, in solution, a multi-component "supercomplex" with the cation. Formation of the complex in the extraction system proceeds spontaneously *via* a self-assembly mechanism. Inner shell of these complexes contains encapsulated metal particle bonded to polar donor atoms, outer shell of the "supercomplexes" is composed by hydrophobic hydroborate core. The charge of the cation is then fully compensated by the inherent negative charge of several particles of the extractant, and the hydrophobic electroneutral supercomplex is pulled into organic phase. With the increasing number of hydrophobic anion particles involved in the complex, the tendency for the transport to the organic phase would increase. The validity of this principle (i.e. 3:1 complex formation for M^{3+} and its transfer to organic phase, schematically depicted on Figure 3), was confirmed by extraction results, and a recent electrochemical study [9].

Figure 3. **Schematic drawing of the complex particle formation**

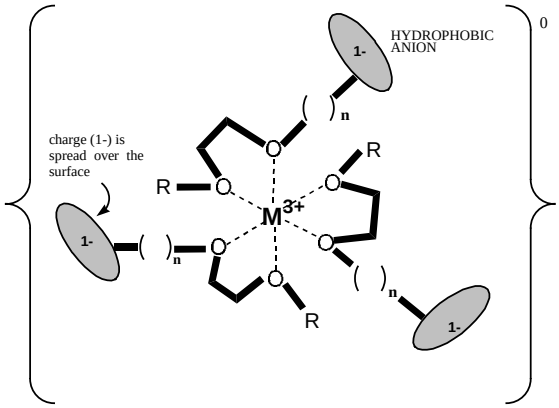

A significant advantage of COSAN lies also in remarkable flexibility of its possible substitution modifications by groups behaving as mono- to poly-donors.

Synthetic strategies to most of such compound have been based on 8-dioxane-COSAN (**10**) [10] derivative ring opening procedure by a suitable organic base, deprotonized *in situ* using NaH (see Figure 4). This method seems synthetically the most feasible, efficient, and high-yield way for synthesis of series of COSAN based anionic species with solvent extraction properties (SER). The series of organic terminal groups successfully attached on COSAN *via* compound **10** dioxane ring opening include: 1.t-Octylphenoxide (**11**), 3-CF_3-phenoxide (Trifluorocresol) (**12**), 2-Benzyl-phenoxide (**13**), 2-phenylphenoxide (**13**), 2-MeO-phenoxide (Guaiacol) (**14**), $[(BUO)_2P = O]^-$ (**15**) and $[(PhO)_2P = O]^-$ (**16**) (last two as an end-group with powerful sequestering properties). Recently, also diphenylphosphine oxide moiety has been chosen for its well-known properties to act, even alone, as efficient sequestering agents for lanthanides and actinides. The species containing the $Ph_2P(O)$ (**17**) moiety as terminal group bonded on the diethyleneglycol chain was prepared *via* reaction of $NaPPh_2$ with COSDIOX and subsequent air oxidation of the zwitterionic intermediate by air. All SER of this type are capable to transfer the target ions (M^{3+}) from aqueous solution into aromatic hydrocarbons without any other additives.

Figure 4. **Schematic drawing of the general route leading to the synthesis of anionic species 11-21**

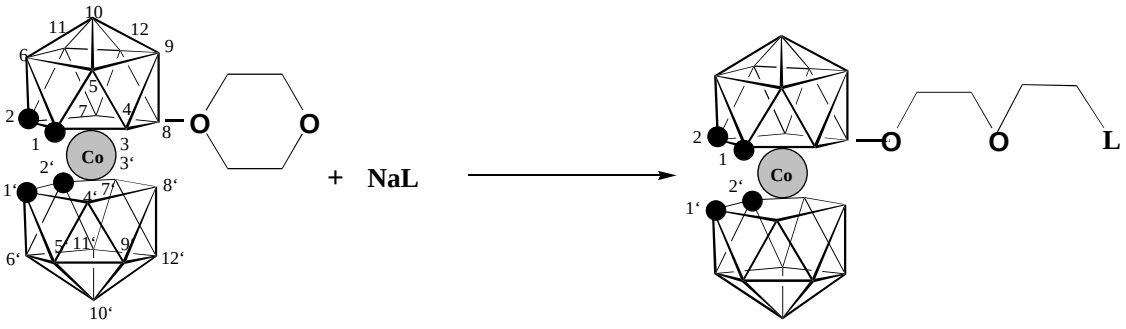

COSANdioxanate

On the other hand, all the above anions (**11-17**) have proved to be effective Eu^{3+} extractants only under neutral or slightly acidic conditions. No one of the investigated SER of this type seemed promising for technological application in strongly acidic medium. The unfavourable dependence on pH could be explained in terms of protonation of a strongly basic oxygen $B_{(8)}$-O-R leading to a $[SER^{(-)}. H^{(+)}]$ "zwitterion", no longer capable to sequester the target ion and especially to compensate its (+) charge. To test this idea, the low efficient dibutyl ester **15** was converted *via* alkaline hydrolysis to the PHOSDIOX with the monobutyl ester of phosphonic acid (**18**) as the terminal group and after complete hydrolysis to PHOSDIOX Acid (**19**) with $–P(O)(OH)_2$ group on the spacer chain. Indeed, these compounds were found reasonably more effective and amazingly specific for Eu^{3+}. However, a decrease of D_{Eu3+} values with increase of HNO_3 concentration could still be seen (see Tables 1 and 2).

From the study made on a series of model, purely organic phosphonic acid derivatives followed: the oxygen in the spacer arm between COSAN and phosphorus containing moiety plays no role in sequestration of the Eu^{3+} -ion. Probably the acidity of the end group and its donating properties are decisive for cation binding.

Table 1. **Extraction of some fission products by PHOSDIOX extractant 18**

C_{HNO3}	D_{Cs}	D_{Sr}	D_{Eu}
0.01	50.5	10.9	9.98
0.03	–	–	36.5
0.05	–	–	191
0.08	–	–	847
0.11	6.18	0.22	1519
0.31	–	–	160
1.01	0.368	0.004	1.94
2.01	0.113	–	0.252
3.01	0.047	–	0.111

0.05 M PHOSDIOX in toluene (obtained solution), up to 0.05 M HNO_3 some reagent losses to the aqueous phase.

Table 2. **Europium extraction by PHOSDIOX acid 19**

C_{HNO3}	0.01	0.05	0.11	0.51	1.01	1.51	2.01	3.01
D_{Eu}	111	2 376	4 959	63.1	3.99	1.32	0.45	0.08

0.05 M PHOSDIOX acid in toluene, in all cases reagent losses to the aqueous phase.

Two compounds of the above type with (CH_2-15-crown-5) (**20**) and (CH_2-21-crown-7) (**21**) terminal groups bonded *via* diethyleneglycol chain were prepared and tested. Especially the last compound exhibits good selectivity and enhanced extraction properties for Sr^{2+}.

More recently, new synthetic methods for direct attachment of phosphorus containing substituents on COSAN cage have been successfully developed starting from COSAN-OH (**22**) and COSAN-$(OH)_2$ (**23**). The ancient synthetic procedures [11] leading to hydroxyderivatives of COSAN were revised and substantially improved. The species **22** and **23** were used as useful synthons for bonding a large variety of metal selective phosphorus containing groups on the cage. Non bridged 8-$(HO)_2$PO-O- COSAN acid

(**24**), 8-PhPO(OH)-O-COSAN (**25**), and bridged 8,8'-μ-HO(O)P(O)$_2$COSAN (**26**) and 8,8'-μ-Ph(O)P(O)$_2$-COSAN (**27**) anions containing phosphorus moiety were prepared in amounts sufficient for testing. Further attention has been paid to improve their extraction properties and the solubility in less polar solvents. Compound containing the bridging diethylphosporamide (**28**) moiety was synthesised and characterised.

Figure 5. **Examples of anionic compounds with non bridged 23 and bridged 25 B-O-P bonded phosphorus containing selective group**

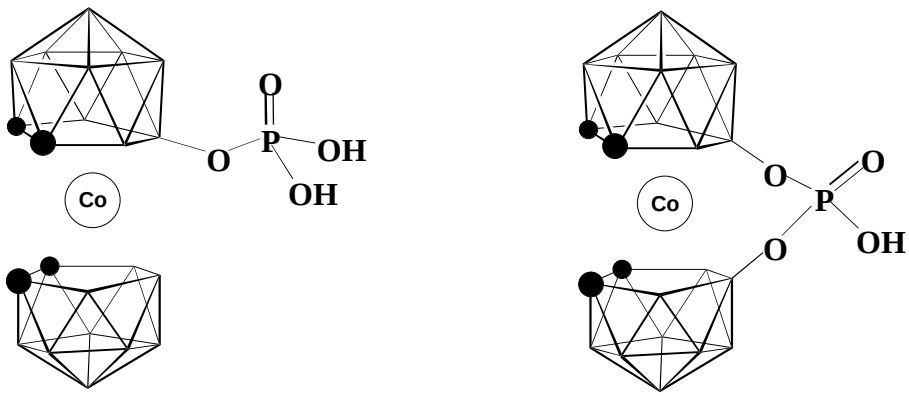

24

From the standpoint of Eu^{3+} extraction neither non-bridged phosphoric acid derivatives **24, 25** nor their bridged analogue **27** were exceptionally effective reagents. Best extraction results have been observed with the species **26** with the -8,8'-O_2>P(O)(OH) bridge substituent, which has been found efficient in europium extraction (see data in Tables 3 and 4). This compound exhibit maximum on nitric acid concentration dependence of Eu^{3+} extraction, the maximum distribution ratio being over 10^3 at 0.2M HNO_3 then falling down but still sufficiently high at 1 M concentration.

Table 3. **The Eu extraction by different bridge-type extractants 26-28**

C_{HNO3}	D_{Eu}						
	0.1	0.3	0.5	1.0	2.0	3.0	5.0
26	158	61.6	16.0	4.79	0.910	0.462	0.247
27	32.2	–	–	0.124	–	–	–
28	45.7	29.9	–	4.82	1.55	–	–

0.01 M extractant in xylene.

Table 4. **Acid dependence on europium extraction by phosphoric acid bridged COSAN 26**

C_{HNO3}	0.01	0.03	0.05	0.1	0.3	1.0	3.0
D_{Eu}	157	157	363	158	61.1	4.79	0.46

0.01 M compound 26 in xylene.

All compounds presented above were adequately characterised by HPLC, FAB M.S., high field multinuclear NMR and some of them by X-ray diffraction. The structures of all extraction reagents were presented at the meeting, along with comprehensive extraction tests results.

General drawback of nearly all mentioned – otherwise successful – extractants still seems to be their not sufficiently high solubility in low polar solvents. It is believed that further substitution of their molecules can increase their hydrophobicity and solubility in solvents of interest. The development of new possible extractants still continues within the framework of the EEC Project. Therefore more efficient extractants could be found, which technology should be developed in the future. According to the last results, a solution could be reached, COSAN extractants developed very recently on the similar basis provided D_{Eu3+} extraction coefficient in the order of hundreds from standard waste solution (1M HNO_3 + 4M $NaNO_3$) using 0 01 M extractant and either toluene or xylene as the solvent.

Up to date, the samples of extractants were prepared in several gram quantities. If the process based on their use is accepted for technological use, Katchem Prague, Ltd. is supposed to be their main producer, and the technology of large scale production scale should be developed and optimised in co-operation with IIC.

Acknowledgements

The partial support from EEC Project IC-CT-155-221, the Grant Agency of the Czech Republic (Grant 104-99-1096) and the grant of Czech Ministry of Education OK 429(2000) was highly appreciated.

REFERENCES

[1] Kyrš M., Heřmánek S., Rais J., Plešek J., Czechoslovak Patent 182 913 (11.02.1972).

[2] Selucký P., Baše K., Plešek J., Heřmánek S., Rais J., Czechoslovak Patent 215282 (01.08.1981).

[3] Rais J. Selucký P., Kyrš M., J. Inorg. Nucl. Chem. 1976, 38, 1376.

[4] Plešek J., Heřmánek S., Czechoslovak Patent 188587 (04.11.1981).

[5] Romanovsky V.N., Proceedings of the 5th International Information Exchange Meeting on Actinide and Fission Product Partitioning and Transmutation, Mol, Belgium, Nov.25-27, 1998, EUR18898 EN, pp. 77-85, OECD/NEA (Nuclear Energy Agency), Paris, France, 1999.

[6] Lazarev L.N., Lyubtsev R.I., Galkin B.Ya., Romanovsky V.N., Shishkin D.N., Kyrš M., Selucký P., Rais J., Heřmánek S., Plešek J., USSR Patent 1031088 (06.06.1981).

[7] Final Report, Project CIPA-CT93-0133, European Commission, February 1997.

[8] Plešek J., Heřmánek S., Collect. Czech. Chem. Commun., 1995, 60, 1297-1302.

[9] Mareček V., Jäncherova J., Plešek J., Grüner B, Paper under preparation.

[10] J. Plešek, S. Heřmánek, A. Franken, I. Císařová and Ch. Nachtigal, Coll. Czech. Chem. Commun., 1997, 62, 47.

[11] Francis J.N., Hawthorne M.F., Inorg. Chem. 1971, 10, 594.

INFLUENCE OF INTERMEDIATE CHEMICAL REPROCESSING ON FUEL LIFETIME AND BURN-UP

A.S. Gerasimov, G.V. Kiselev, L.A. Myrtsymova
State Scientific Centre of the Russian Federation
Institute of Theoretical and Experimental Physics (RF SSC ITEP)
25, B. Cheremushkinskaya, 117259 Moscow, Russian Federation

Abstract

The influence of intermediate chemical processing of nuclear fuel with removal of fission products on the fuel burn-up and lifetime for heavy water CANDU type reactors operating with fuel on base of natural uranium is studied in this paper. Two types of nuclear fuel are considered: natural and slightly enriched uranium (with enrichment up to 1.4%) and thorium fuel on basis of ^{232}Th-^{233}U. Intermediate chemical processing permits to prolong lifetime and to increase fuel burn-up. However, the effect is not so high, the increase of burn-up is about 20%. More effect is gained by use of a fuel with increased enrichment.

1. Introduction

A heavy-water CANDU-type reactor has good neutron-physical characteristics due to the use of heavy water as moderator and coolant. In particular, it allows using natural uranium as nuclear fuel, whereas in other types of thermal neutron reactors, it is necessary to use uranium with enrichment of several percents. In natural uranium fuel, the relative role of plutonium produced from ^{238}U is great. Nevertheless, fuel burn-up and lifetime are small because fuel multiplying properties at burning out are quickly reduced. One of the opportunities to increase the lifetime is the transition to nuclear fuel with slight enrichment. Another opportunity, intermediate chemical processing of fuel can be considered where the fission products are removed and fuel nuclides are recycled for further burning.

For the future atomic power, a nuclear fuel cycle on base of ^{232}Th-^{233}U can be rather perspective. Thorium cycle has essential advantages over traditional uranium – plutonium cycle because of considerably less amount of transuranium long-lived radioactive wastes (though considerably more amount of rather harmful ^{232}U). In CANDU reactors, operation in thorium cycle and, the intermediate fuel cleaning of the fission products could also prolong lifetime and lower the requirement of specially obtained ^{233}U.

In this paper, results are given of a calculation study of the influence of intermediate chemical processing of nuclear fuel with removal of fission products on fuel lifetime and burn-up in CANDU-type reactor are given. Uranium fuel on basis of natural and slightly enriched uranium (with enrichment up to 1.4%) and thorium fuel on base of ^{232}Th-^{233}U are considered.

2. Calculation model

The reactor design is described in [1]. In an active core, 380 fuel assemblies are placed. Every assembly contains 37 uranium pins with zirconium cladding in zirconium tube. Heavy water is used as the coolant and moderator. Fuel assemblies are located in a square lattice with a pitch of 23.5 cm. Height of an active core is 594 cm. Natural uranium loading in reactor is 114 tonnes.

It was accepted in calculations that reactor multiplying properties can be approximately described by multiplication factor of an elementary cell as follows. Multiplication factor of an elementary cell k_{eff} varies in function of fuel burn-up. The reactor operates in a mode of continuous refuelling. Fuel assemblies with various burn-up from fresh fuel up to maximum burn-up are situated in core at every moment. The on-load refuelling is carried out independently in different channels after achieving the maximal burn-up. It allows accepting the value of multiplication factor in an elementary cell $<k>$ average over fuel lifetime with correction on neutrons leakage from reactor as approximate reactor multiplication factor. Such approximation is quite justified for comparative calculations of the effect of intermediate nuclear fuel cleaning.

At calculations of lifetime, it was considered that the neutrons leakage makes 1% and the value $<k> = 1.01$ was accepted.

In reactors with continuous refuelling at constant power, the value of neutron flux varies in time very slightly. It is necessary that the power of one fuel assembly varies in time because of changing of fissile nuclide amount, and the fuel assemblies with different burn-up have appreciably different power. Calculations of fuel burn-up and transformation of isotopes were carried out at constant neutron flux.

3. Natural or slightly enriched uranium fuel

The calculations of reaction rates and multiplication factor in an elementary cell were performed with the code [2]. A fuel assembly with pins was represented as a 4-ring coaxial assembly with the same volumes of all-structural materials and fuel loading. The enrichment of uranium from 0.714% up to 1.4% was considered. The amount of uranium in fresh fuel assembly was accepted the same for all enrichments, and the ^{235}U amount corresponded to the enrichment. For natural uranium fuel, thermal neutrons flux was equal to $\Phi = 5\ 10^{13}$ n/cm^{2}s. Neutron flux for the enriched fuel was determined in a way to get the same power of fresh fuel assembly as in the variant with natural uranium. At calculations of nuclide transformation, isotopes of uranium, neptunium, plutonium, americium and curium up to ^{244}Cm were taken into account.

In uranium fuel, ^{239}Pu is produced. This isotope gives the essential contribution in reactivity of CANDU-type reactor with natural or slightly enriched fuel already in the initial period of fuel lifetime. The dependence of multiplication factor k_{eff} in an elementary cell on irradiation time T was calculated for initial enrichment of uranium from 0.714% up to 1.4% without intermediate cleaning. The neutron capture by fission products was taken into account by means of an "effective fission fragment" [3]. A poisoning by ^{135}Xe, ^{105}Rh and absorption of neutrons by ^{149}Sm and ^{151}Sm were additionally taken into account. The fuel lifetime T_f was determined by value <k> = 1.01. Table 1, fuel lifetime T_f and burn-up FP defined by amount of fission products in 1 tonne of fuel without intermediate cleaning for different initial uranium enrichment C.

Table 1. **Fuel lifetime T_f and burn-up FP without intermediate cleaning**

C, %	0.714	1.0	1.2	1.4
T_f, years	2.0	2.8	5.38	6.67
FP, kg/tonne	11.4	17.4	20.8	23.4

Analogous time dependence of multiplication factor in an elementary cell k_{eff} with intermediate processing with cleaning from accumulated fission products was calculated for natural uranium fuel and fuel with enrichment 1%. The intermediate processing was carried out at time T_p = 0.8, 1.2, 1.6 years. For enrichment 1%, the intermediate processing was carried out also at T_p = 2 and 2.4 years. These data allow to estimate fuel lifetime corresponding to average over lifetime multiplication factor <k> = 1.01. They are presented in Table 2. T_p = 0 corresponds to the mode without intermediate cleaning.

Table 2. **Fuel lifetime T_f and burn-up FP with intermediate processing**

T_p, years	**C = 0.714%**		**C = 1.0%**	
	T_f, years	FP, kg/ton	T_f, years	FP, kg/ton
0.0	2.0	11.4	3.9	17.4
0.8	2.52	13.8	4.71	19.9
1.2	2.4	13.3	4.76	20.1
1.6	2.4	13.3	4.69	19.8
2.0	–	–	4.57	19.5
2.4	–	–	4.41	19.0

These data show that fuel lifetime and burn-up in modes without intermediate processing essentially depend on fuel enrichment. At transition from natural uranium to enrichment 1%, the lifetime is increased 1.95 times (and 1.4 times because of reduction of flux density necessary to obtain the same power of fresh fuel assembly) and the burn-up grows 1.5 times. At transition from natural uranium to enrichment 1.4%, the lifetime is increased 3.3 times and the burn-up grows 2 times. In variants with intermediate processing, the lifetime increase is not so high. The maximal lifetime for natural uranium, 2.52 years, and burn-up, 13.8 kg/tonne, correspond to time point of processing T_p = 0.8 years. The lifetime is longer by 26% and burn-up is greater by 21% than without intermediate processing. For 1% enrichment, the maximal lifetime is 4.76 years and burn-up makes 20.1 kg/tonne. Processing will be done at T_p = 1.2 years. The increase in lifetime is 22% and that of in burn-up is 16% in comparison with a mode without processing.

4. Thorium fuel ^{232}Th-^{233}U

In thorium mode of operation, all fuel assemblies were considered alike, containing identical fuel on basis of ^{232}Th and ^{233}U. The same elementary cell was studied as for uranium fuel. The thorium amount in fuel zones was accepted the same as ^{238}U in uranium fuel. The share of ^{233}U in fresh fuel was chosen 1.96% with respect to the amount of ^{232}Th. That has ensured necessary over-criticality of a cell for appropriate fuel lifetime and burn-up.

During calculation of nuclide transformation, the production of isotopes of protactinium, uranium, neptunium, plutonium up to ^{242}Pu was taken into account. The neutron flux is considered constant over a lifetime and equal to $5 \cdot 10^{13}$ neutr/cm^{2}s. In modes with intermediate processing, it was considered that short-lived ^{233}Pa at an intermediate reactor shutdown completely decays into ^{233}U. The intermediate processing is made at time points T_p = 0.4, 0.8, 1.2 years. Fuel lifetime and burn-up corresponding to <k> = 1.01 for different points of intermediate cleaning are shown in Table 3.

Table 3. **Fuel lifetime T_f and burn-up FP in thorium modes**

T_p, years	T_f, years	FP, kg/ton
0	1.45	9.5
0.4	1.71	11.1
0.8	1.75	11.3
1.2	1.72	11.1

The lifetime without intermediate cleaning makes 1.45 years, burnup is 9.5 kg/ton. The maximal increase of fuel lifetime and burn-up at the expense of intermediate processing in comparison with a usual mode is achieved at processing at T_p = 0.8 years and makes about 20%.

5. Conclusion

The research performed has allowed to establish how it is possible to extend lifetime and to increase fuel burn-up at the expense of increase of uranium enrichment or at the expense of intermediate processing of uranium and thorium fuel with fission products removal. If a power of fresh fuel assembly remains constant with increase of uranium enrichment, it is necessary to reduce the neutron flux. At the expense of this effect, the lifetime is extended even at the same burn-up of fuel. Increase of burn-up and additional lifetime increase are caused by reactivity rise. At transition from natural uranium to

enrichment 1%, the burn-up grows 1.5 times, the lifetime is extended 1.95 times from 2 up to 3.9 years, the burn-up corresponding to natural uranium is achieved after 2.24 years. At transition from natural uranium to enrichment 1.4% the burn-up grows 2 times, the lifetime is extended 3.3 times. In modes with intermediate cleaning of fission products, an increase of lifetime is not so high. The lifetime for natural uranium raises by 26%, burn-up by 21%. For 1% uranium, an increase of lifetime is 22% and that of burn-up is 16%. The optimum time point of processing is somewhat less than half of lifetime without processing. In thorium mode, the maximal increase of fuel lifetime and burn-up at the expense of intermediate cleaning in comparison with a usual mode makes about 20%. Thus, the increase of burn-up and lifetime are obtained much more effectively at the expense of fuel enrichment.

REFERENCES

[1] *Karachi Nuclear Power Plant*, In: Directory of Nuclear Reactors. Vol. IX, Power Reactors. IAEA, Vienna, 1971, pp. 167-174.

[2] A.Ya. Burmistrov, B.P. Kochurov, *Space-energy Neutron Distribution in Cylindrical Cell of a Reactor (Code TRIFON)*, Moscow, Pre-print ITEP, 1978, #107.

[3] A.D. Galanin, *Introduction in the Theory of Nuclear Reactors on Thermal Neutrons*, Moscow, Energoatomizdat, 1990, pp. 362-367.

RECENT PROGRESSES ON PARTITIONING STUDY IN TSINGHUA UNIVERSITY

Chongli Song, Jingming Xu
Institute of Nuclear Energy Technology, Tsinghua University
100084 Beijing, China

Abstract

Recent progresses on partitioning studies in Tsinghua University are reviewed. Declassification of the commercial HLLW to a waste that is suitable to shallow land disposal is possible. An enhanced TRPO process with optimal process parameters can meet the required DF of TRU elements. A Total Partitioning process for commercial HLLW was developed by modification of the TP process for Chinese HLLW. The Total Partitioning process for commercial HLLW consists of an enhanced TRPO process to remove TRU elements and ^{99}Tc, a CESE process to separate strontium, a KTiFC ion exchange process to segregate cesium and an An/Ln separation process with HBTMPDTP. The flow sheet of the total partitioning process for commercial HLLW was given.

1. Introduction

The final disposal of radioactive waste is one of the key problems that effect the development of nuclear energy industry. Partitioning and Transmutation (P&T) concept [1] involves chemical separation of transuranium (TRU) elements as well as long-lived nuclides (for example, ^{99}Tc, ^{129}I, etc.) from HLLW, and transmutation of them to either stable or short-lived nuclides. The P&T constitutes an advanced nuclear fuel cycle. The implementation of the P&T could significantly reduce long-term risk of the radioactive waste.

The partitioning of HLLW can also be used as a pre-treatment method of HLLW to reduce α-waste and HAW volume. In recent years a clean use of nuclear energy (CURE) concept was proposed for the back-end of nuclear fuel cycle [2]. In the CURE concept the partitioning requires not only to remove the TRU, ^{99}Tc and ^{129}I, but also to segregate ^{90}Sr and ^{137}Cs from HLLW. After partitioning the original HLLW would be de-classified to a non-α, low and intermediate lever radioactive waste that could be suitable for shallow-land disposal. So for the CURE concept the required decontamination factors (DF) for TRU elements will be much higher than that for the P&T concept. The required DF of TRU, ^{99}Tc, ^{137}Cs and ^{90}Sr are given in Table 1 for a typical commercial HLLW. The spend nuclear fuel had a burn-up of 33 000 MWd/tU, a cooling time of 10 years and 99.75% of U and Pu had been removed in reprocessing [3]. In Table 1 the α- waste standard of 4×10^5 Bq/kg is chosen and 0.40 m^3 concrete/tU waste is supposed to be produced after solidification of the declassified liquid waste. In order to get a higher waste volume reduction, the separation of lanthanides (Ln) and actinides are necessary for commercial HLLW. The required DF for TRU elements in Ln fraction should be higher than 2.4×10^5 [4].

Table 1. **The required DF for treatment of typical commercial HLLW to a waste suitable to shallow land disposal**

Nuclides	**Activity in HLLW Bq/tU**	**Chinese standard GB-9132-88 Bq/kg**	**Required DF (Solidify by cementation, 0.4 m^3/tU)**
TRU	1.26×10^{14}	4×10^5	4.0×10^5
^{99}Tc	4.78×10^{11}	–	–
^{90}Sr	2.07×10^{15}	4×10^{10}	71
^{137}Cs	3.01×10^{15}	4×10^{10}	104

In recent years, the study on the partitioning process was carried out in Tsinghua University in order to meet the DF requirement for typical commercial HLLW. The aim is to declassify the HLLW to a waste suitable to shallow land disposal. In this paper the recent progresses on partitioning studies in Tsinghua University will be reviewed. The flow sheet of total partitioning process for commercial HLLW was given.

2. The enhancement of TRPO process for commercial HLLW

A TRPO process was developed in Tsinghua University for removing TRU elements from HLLW [5,6] in 1980s. Hot tests of the TRPO process were carried out with HLLW of WAK in Institute for Transuranium Elements (ITU) at Karlsruhe, Germany in 1993 [7]. The hot test was completed with 24 stages of miniature centrifugal contactor in hot cell. The DF value of TRU elements obtained in the

hot tests (See Table2) was enough for the P&T requirement. However, it is not sufficient to meet the required DF for CURE project because the TRPO process was designed for P&T project in the period. In recent year, the TRPO process was improved in order to increase the DF values of TRU elements.

Table 2. **The DF of TRU elements, ^{99}Tc and Nd in the TRPO hot tests**

	HNO_3 in feed	**Extraction stages**	**Decontamination factors**						
			^{237}Np	^{238}U	^{239}Pu	Am/^{241}Pu	^{243}Am	^{99}Tc	^{144}Nd
Run 1	0.75	6	12.4	>5 400	>760	>2 800	>900	>1 400	>22 000
Run 2	1.36	10	>4 100	>7 000	>950	>3 200	>760	>1 700	>33 000

Tetra- and hexa-valent TRU elements are highly extracted by 30% TRPO-kerosene. The controlling elements for the removal of TRU elements are trivalent americium and curium. The extraction behavior for Am and Cm is very similar. So improving Am extraction is a key issue. A simplified optimised objective function [8] was introduced into the TRPO mathematical model for americium extraction [9]. The objective function was designed as that the second waste from the TRPO process should have a minimal volume to improve the safety, cost and to decrease the environmental impact. In addition, in the calculation, the Am decontamination factor should be above 4.0×10^5 and for a conservative consideration, the DF of 4.0×10^6 for Am was fixed. The acidity of feed and scrub solution was chosen to improve neptunium extraction, and was 1.35 M and 0.5 M respectively. The optimal parameters of the TRPO process for Am extraction were obtained [8] and are listed in Table 3.

A multistage counter current cascade experiment with simulated HLLW skipped with ^{241}Am was carried out to verify the calculated results [10]. A set of 20 stages miniature centrifugal extractor was installed in a glove box. Optimal parameters were used in the process experiment (see Table 3). The cascade included 12 stages for extraction, 2 stages for scrubbing and 6 stages for Am stripping. The simulated feed solution had a specific volume of 1 850 L/tU and skipped americium with a specific activity of 7.83×10^6 Bq/ml. The flow ratio of feed/organic/scrub/stripping was 1/1.21/0.265/1.21.

Very good results were obtained in the cascade experiments [10]. The obtained DF_{Am} was 1.25×10^6 and the material balance for Am was 92.6% in the experiments. The americium profiles in each stage are given in the Figure 1. The experiments show that the calculated results fit with the experimental ones very well. The required DF for treating typical commercial HLLW to a waste, that is suitable for sallow land disposal, can be reached with the TRPO process.

Table 3. **Calculated and experimental parameter of the TRPO process (For a typical HLLW of a burn-up of 33 000 MWd/tU, Calculated $DF_{Am} = 4.0 \times 10^6$)**

Parameter	Calculated value[8]	Experimental value [10]
Specific volume of Feed (*F*)	1 750 L/tU	1 875 L/tU
Volume of 30%TRPO-kerosene	1.18 *F*	1.21 *F*
Volume of scrubbing solution	0.267 *F*	0.265 *F*
Volume of stripping solution	1.18 *F*	1.21 *F*
Number of extraction stages	10	10
Number of scrubbing stages	2	2
Number of stripping stages	–	6
HNO_3 concentration in feed solution	1.35 mol/L	1.35 mol/L
HNO_3 concentration in scrubbing solution	0.5 mol/L	0.5 mol/L
HNO_3 concentration in stripping solution	–	5.0 mol/L

Figure 1. **Americium activity profiles in TRPO process**

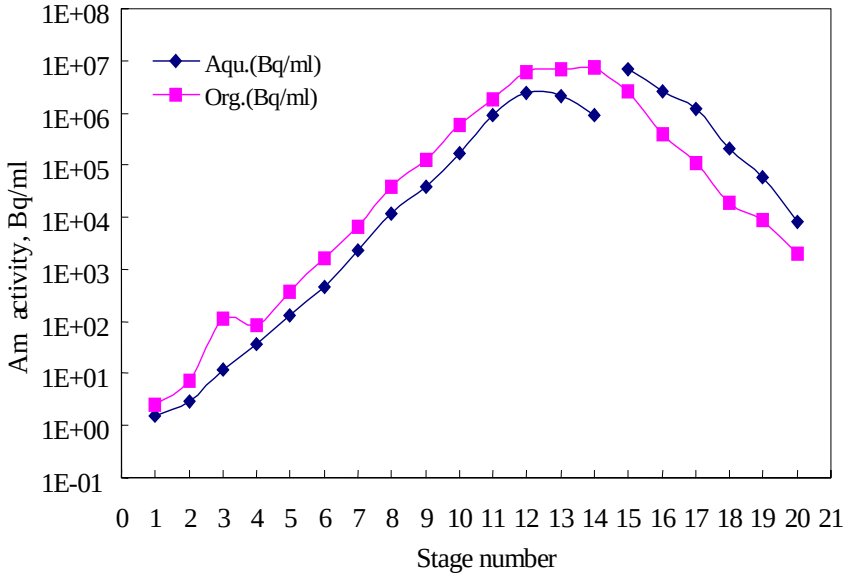

3. The separation of lanthanide and actinides

The separation of trivalent lanthanide (Ln) and actinides is a difficult subject in the separation chemistry. However the separation of Ln and Actinides is necessary no matter how for the P&T concept or for the CURE concept. The study on the separation chemistry of lanthanide and actinides is one of research subjects in Tsinghua University.

An S-coordinated extractant bis (2,4,4 trimethylpentyl) dithiophospninic acid (HBTMPDTP) had been proven to be an effective extractant for the separation of trivalent Am from Ln [11]. The HBTMPDTP is prefers to extract Am rather than Ln and the separation factor reaches to 5 000 for

trace amount of Am and Eu. The HBTMPDTP (>99% purity) was obtained by purification of a commercial extractant Cyanex 301 [12]. The extraction chemistry of Am and Ln was studied with HBTMPDTP. An empirical model of distribution ratio for Am and Ln was derived and a computer program for counter current separation of Am/Ln by HBTMPDTP extraction was compiled [13]. The An/Ln separation process parameters were calculated and were verified by batch multistage counter current extraction experiments.

A conceptual Am/Ln separation flow sheet by HBTMPDTP extraction was proposed for the Am/Ln fraction from partition process of HLLW [14]. The feasibility of the separation flow sheet was verified with a hot test of crossing flow extraction [15]. Am specific activity of was 2×10^5 Bq/ml and the lanthanide concentration was 0.021M in the feed solution. After denitration to 0.3 M HNO_3, the feed solution was first extracted by Cyanex 301 to remove impurities. It was adjusted to pH 3.5 and was then fed into extraction unit. More than 99.999% of Am was extracted into the organic phase with 4 stages of cross extraction. The Am concentration in the raffinate was 1 Bq/ml. Only ~3% Ln was extracted by HBTMPDTP. The average separation factor between Am and Ln was 3 500 for first three stages. The hot test results proved that the separation process was effective.

The synergic extraction and separation of Am and Ln by HBTMPDTP/TBP-Kerosene was also studied. At pH about 2.8, quite high separation factor for Am/Ln could be obtained. A multistage counter current cascade experiment was performed. It included 7 stages for extraction, 3 stages for scrubbing and 2 stages for stripping. Americium was effectively separated from Ln. The separation factor of Am from Ln was 5×10^4 and the separation factor of Ln from Am was 2500 [16].

4. The Total Partition process for commercial HLLW

A Total Partition (TP) process was developed in Tsinghua University during 1990s for Chinese high saline (defence) waste [17,18]. The TP process consists of the TRPO process to remove TRU elements, a Crown extraction process (CESE) to separate strontium and a potassium titanium ferrocyanide (KTiFC) ion exchanger to segregate caesium. After the treatment by the TP process, the high saline HLLW was declassified to a non-α low and intermediate waste, that could be cementation and sallow land disposal. The hot test proved that the TP process worked very well for the waste.

In commercial HLLW, the salt content is much lower than that in the high saline HLLW. Low salt content benefits the TRU extraction by TRPO extractant. However, it is detrimental to the strontium extraction by crown ether $DCH_{18}C_6$. This problem can be solved by addition a concentration and denitration unit between the TRPO and the CESE process. The unit was used for increasing the salt content by evaporation and then to adjust the acidity of the solution. The crown ether extraction and the KTiFC ion exchanger can meet the required DFs of strontium and cesium for commercial HLLW. The hot test of the TP process for Chinese HLLW had proved the fact. So the TP process for high saline HLLW can also be used for commercial HLLW after modification. The general flow sheet of the TP process for commercial HLLW is given in Figure 2. In the flow sheet, the An/Ln separation process is also included.

Figure 2. **General flow-sheet of Total Partition process for commercial HLLW**

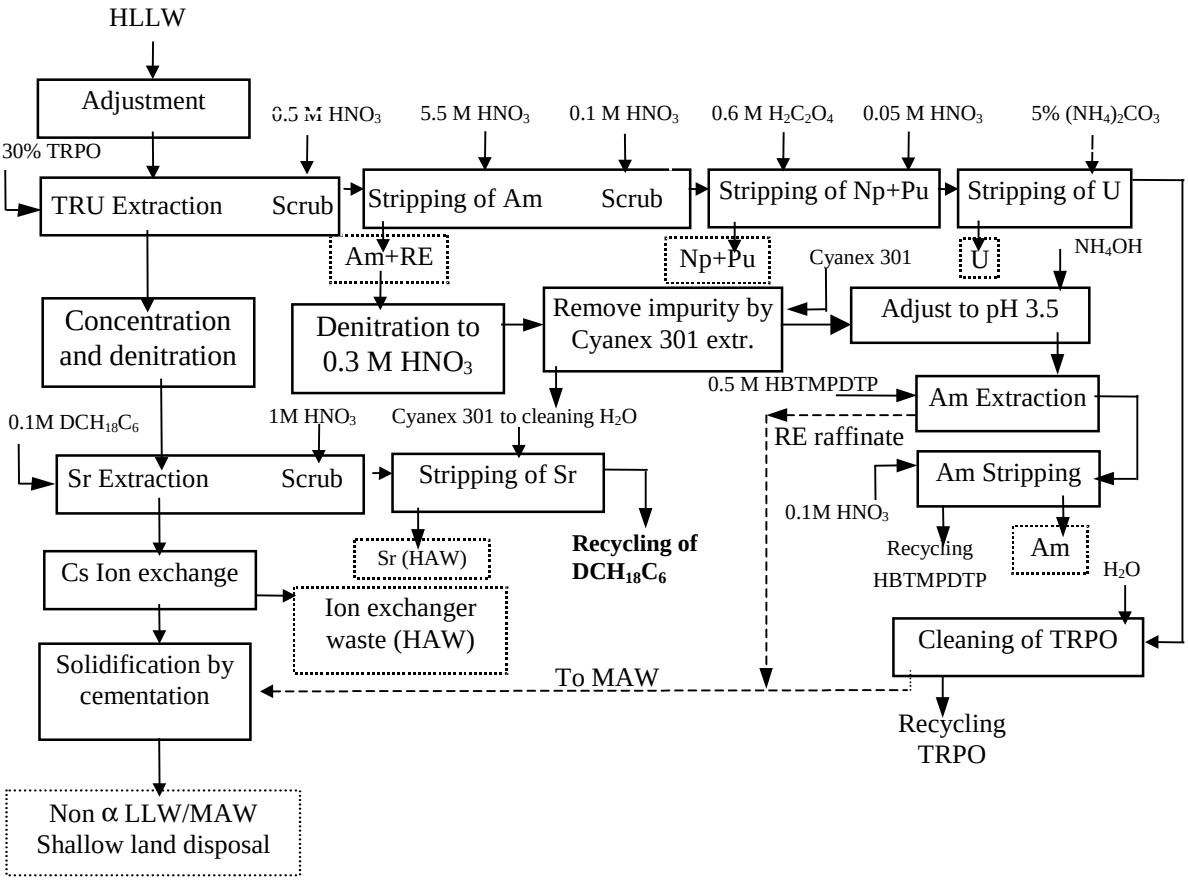

The auxiliary processes of the TP process are now being studied. They include the denitration and calcination for Am (RE) stripping solution, Np/Pu separation in $H_2C_2O_4$-HNO_3 solution, the conversion process for uranium stripping solution and immobilization process for Cs-loaded KTiFC ion exchanger. The advanced extraction equipment such as pulsed column and centrifugal contactor for the TP process are also being studied.

5. The radiation stability of TRPO extractant

The radiation stability of TRPO extractant was studied in recent year. The physical properties of 30% TRPO do not have obvious change between a dose of 1×10^4 to 5×10^5 Gy [19]. Main gaseous radiolytic products and acidic radiolytic products of 30% TRPO-kerosene extractant were analysed. Their radiation yield (G value) was determined [20]. At a dose of 1×10^4 to 1×10^6 Gy, radiolytic products do not have obvious effect on the extraction. When the radiation dose was above 2×10^6, some retention of heave elements were observed [21]. Research indicates that the polymeric products with high molecular weight cause the retention. The studies show that the TRPO extractant is much more stable than TBP.

6. Conclusion

Declassification of the commercial HLLW to a waste that is suitable to shallow land disposal is possible. An enhanced TRPO process can meet the required DF for TRU elements with optimal process parameter. A Total Partition process for commercial HLLW was developed by modification of the TP process for Chinese HLLW. It consists of an enhanced TRPO process to remove TRU elements and ^{99}Tc, a CESE process to separate strontium, a KTiFC ion exchange process to segregate caesium and an An/Ln separation process with HBTMPDTP.

REFERENCES

[1] A.C. Croff, J.O. Blomeke, *Actinide Partitioning-Transmutation Program*, Final Report, ORNL 5566 (1980).

[2] S.E. BINNEY, *CURE: Clean Use of Reactor Energy*, WHC-EP-0206 Westinghouse Hanford Company, Richland, WA 99352, 1990.

[3] C. Song, *Study on Partitioning of Long Lived Nuclides from HLLW in Tsinghua University*, in Energy Future in the Asia/Pacific Region, Proceeding of the International Symposium, Beijing, China, 2000, pp. 89-99.

[4] Y. Zhu, J. Chen, R. Jiao, *Hot Test and Process Parameter Calculation of Purified Cyanex 301 Extraction for Separating Am and Fission Product Lanthanide*, Proceedings of the Global'97 Conference, Yokohama, Japan, 1997, Vol. 1, pp. 581-585.

[5] Y. Zhu and C. Song, *Recovery of Neptunium, Plutonium and Americium from Highly Active Waste, Tri-alkyl phosphine Oxide Extraction, in Transuranium Elements: A Half Century*, Edited by L.R. Morss and J. Fuger, 1992, ACS, Washington D.C. USA, pp. 318-330.

[6] C. Song, Y. Zhu, D. Yang, L. He, J. Xu, Chinese J. Nucl. Sci. Eng., 1992, 12 (3), 225 (in Chinese).

[7] J-P. Glatz, C. Song, L. Koch, H. Bokelund, H. He, *Hot Tests of the TRPO Process for the Removal of TRU Elements From HLLW*, Proceedings of the Global'95 Conference, Versailles, France, 10-14 Sept.1995, Vol. 1, pp. 548.

[8] J. Chen, J. Wang, C. Song, *Optimization of TRPO Process Parameters for Americium Extraction*, to be published in Tsinghua Science and Technology, 2001 (in English).

[9] C. Song, J.-P. Glatz, *Mathematical Model for the Extraction of Americium from HLLW by 30% TRPO and its Experimental Verification*, in A Value Adding Through Solvent Extraction: International Conference on Solvent Extraction, Vol. 2, The University of Melbourne, Australia, 1996.

[10] J. Wang, B. Liu, J. Chen, C. Song, R. Jiao, G. Tain, X. Liu, R. Jia, *Test of Removing Americium From Simulated Commercial High Level Liquid Waste*, to be published in J. Tsinghua University (Science and Technology) (in Chinese).

[11] Y. Zhu, J. Chen, R. Jiao, *Extraction of Am(III) and Eu(III) from Nitrate Solution With Purified Cyanex 301,* Solv. Extr. & Ion Exch. 1996, 14, pp. 61.

[12] J. Chen, R. Jiao, Y. Zhu, *Purification of Cyanex 301 and its property*, Chinese J. Applied Chem. 1996, 13(2), 46 (in Chinese).

[13] J. Chen, Y. Zhu, R. Jiao, *Separation of Am(III) from Fission Product Lanthanide by bis(2,4,4-trimethyl pentyl) dithiophosphinic Acid Extraction – Process Parameters Calculation,* Nuclear Technology, 1998, 122, pp. 64.

[14] J. Chen, R. Jiao, Y. Zhu, *A Conceptual Flow Sheet for Am/Ln Separation by HBTMPDTP Extraction,* to be published.

[15] J. Chen, R. Jiao, Y. Zhu, *A Cross-flow Hot Test for Separating Am From Fission Product Lanthanide by bis(2,4,4-trimethylpenthyl) dithiophosphinic acid*, Radiochimica Acta, 1997, 76, pp. 129.

[16] X. Wang, Y. Zhu, R. Jiao, *Separation of Am from Lanthanides by a Synergistic Mixture of Purified Cyanex 301 and TBP*, to be published in J. Radioanal. Nucl. Chem.

[17] C. Song, *The Concept Flow Sheet of Partitioning Process for the Chinese High-level Liquid Waste,* Atomic Energy Science and Technology, 1995, 29, 201-9 (in Chinese).

[18] C. Song, J. Wang, R. Jiao, *Hot Test of Total Partitioning Process for the Treatment of High Saline HLLW*, in Global'99: International Conference on Future nuclear systems, Proceedings, August 29-September 3, 1999, Jackson Hole, USA.

[19] R. Xin, P. Zhang, J. Liang, C. Song, *Study on the Radiation Stability of Trialkyl Phosphine Oxide*, to be published.

[20] R. Xin, C. Song, J. Jiao, J. Liang, *Investigation of Radiolytic Products of Trialkyl Phosphine Oxide by Gas Chromatography*, Chinese J. Spectroscopy Laboratory, 1999, 16, pp. 498-502.

[21] P. Zhang, C. Song, J. Liang, R. Xin, *Extraction and Retention of Plutonium with γ-irradiated 30% Trialkylphosphine Oxide-Kerosene Solution*, to be published in Solv. Extr. & Ion Exch.